



Original article

Guanidine-based α_2 -adrenoceptor ligands: Towards selective antagonist activityDaniel H. O'Donovan ^a, Carolina Muguruza ^b, Luis F. Callado ^b, Isabel Rozas ^{a,*}^a School of Chemistry, TBSI, Trinity Biomedical Sciences Institute, Trinity College Dublin, 152-160 Pearse Street, Dublin 2, Ireland^b Department of Pharmacology, University of the Basque Country UPV/EHU, and Centro de Investigación Biomédica en Red de Salud Mental CIBERSAM, Spain

ARTICLE INFO

Article history:

Received 5 March 2014

Received in revised form

19 May 2014

Accepted 23 May 2014

Available online 27 May 2014

Keywords:

Pharmacophore

Alpha 2-adrenoceptor

Antagonists

Human prefrontal cortex tissue

[³⁵S]GTP γ S

ABSTRACT

Depression has been linked to a selective increase in the high affinity conformation of the α_2 -adrenergic autoreceptors (α_2 -ARs) in the human brain as well as to an overexpression of α_2 -ARs in the hippocampus and cerebral cortex. Thus, the development of novel α_2 -AR antagonists represents an attractive source of new antidepressants. This paper describes the design, synthesis and pharmacological evaluation of 30 new guanidinium and 2-iminoimidazolidinium as potential α_2 -AR antagonists. In order to design this new series of α_2 -AR antagonists, a pharmacophore model was developed using the GALAHAD software. This study suggested that increased substitution in the space surrounding the cationic guanidine moiety might lead selectively to antagonist activity. Following the preparation of compounds incorporating this feature and competitive radioligand binding, [³⁵S]GTP γ S functional assays revealed that this structural modification affords exclusively α_2 -AR antagonists, in contrast with the analogous unsubstituted compounds in which a mixture of antagonist/agonist activities was previously observed.

© 2014 Elsevier Masson SAS. All rights reserved.

1. Introduction

Depression is a mental disorder characterized by a long-lasting low mood, behavioural changes, and increased morbidity and mortality. As a major worldwide health burden, the World Health Organisation has predicted that by the year 2020, depression will constitute the single largest contributor to morbidity and disability in the developed world [1]. Although the complete aetiology remains unclear, depression has been closely linked to changes in monoaminergic neurotransmission [2], and virtually all clinically effective antidepressant drugs have been shown to exert activity upon monoaminergic targets [3].

The α_2 -adrenoceptors (α_2 -ARs) represent one such target, as the activation of presynaptic α_2 -ARs autoreceptors by endogenous noradrenaline (NA) inhibits the release of neurotransmitters into the synapse [4], hence, antagonism of α_2 -ARs results in increased synaptic concentrations of monoamines [5]. Recent studies have

suggested that not only the presynaptic autoreceptors but also the postsynaptic α_2 -ARs may play a role in the activity of some antidepressants [6]. It has also been shown that α_2 -AR activation reduces neurogenesis in the hippocampus, an effect now seen as a fundamental causative factor in depression [7]. As such, α_2 -AR blockade results in increased hippocampal neurogenesis [8]. Interestingly, a selective increase in the high-affinity conformation of α_2 -ARs has been found in the hippocampus and cerebral cortex of patients suffering from depression [9]. Moreover, α_2 -AR antagonists have been shown to induce gene expression of the plasticity-promoting protein Arc, thereby improving neuroplasticity in depressed individuals [10,11]. All these theories strongly support the application of α_2 -AR antagonists as antidepressants.

The antidepressant potential of the α_2 -ARs has been studied since the 1960s when researchers identified the tetracyclic antidepressants mianserin (1) and mirtazapine (2) [12] and attributed their activity to their α_2 -AR antagonism (Fig. 1) [13]. Studies have shown that mirtazapine exhibits a level of clinical efficacy similar to that of the serotonin transporter inhibitor venlafaxine [14], which is the best-selling antidepressant at the time of writing. However, as with other clinically used antidepressants, mirtazapine still presents unwanted side effects and a long onset of action, prompting the need for improved α_2 -AR antagonist antidepressants. It has also been suggested that co-administration of selective α_2 -AR

Abbreviations: α_2 -AR, Alpha 2-adrenoceptor; [³⁵S]GTP γ S, radio labelled guanosine 5'-O-[gamma-thio]triphosphate; pK_i, minus logarithm of the binding constant; [³H]RX821002, 2-methoxyidazoxan; UK14304, Brimonidine; EC₅₀, Half-maximal effective concentration; EGFR, Epidermal.

* Corresponding author.

E-mail address: rozasi@tcd.ie (I. Rozas).

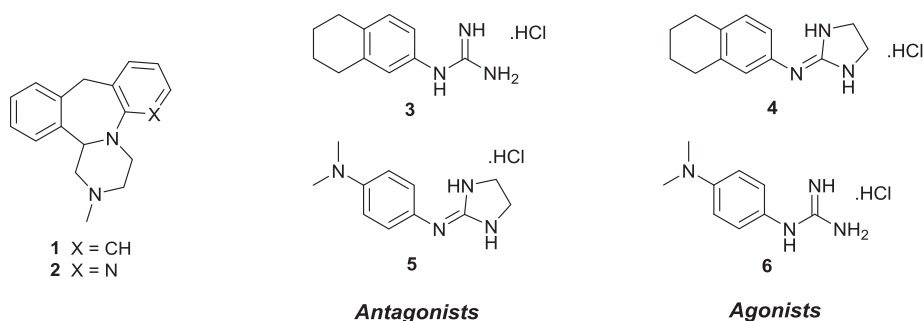


Fig. 1. Structures of α_2 -AR antagonists mianserin (1), mirtazapine (2), compounds 3 and 5 and α_2 -AR agonists 4 and 6.

antagonist drugs might potentiate the effects of noradrenaline and serotonin reuptake inhibitor antidepressants by enhancing extracellular NA concentrations in the brain [15].

Our group has been interested in the development of novel α_2 -AR antagonists since the 2000s, during which time we synthesized and evaluated more than 80 arylguanidinium and aryl-2-iminoimidazolidinium α_2 -AR ligands as potential antidepressants, including animal studies with several promising *in vitro* candidate compounds [16–19]. Although these studies produced a wealth of pharmacological data, it proved difficult to establish definitive structure–activity relationships. For example, guanidine derivative 3 was found to be an α_2 -AR antagonist, while its 2-iminoimidazolidinium analogue 4 behaves as an agonist [17]; however, in the case of compounds 5 and 6 this pattern is reversed [16] (Fig. 1). As such, the question of which structural features might consistently lead to antagonistic activity was of central importance to our efforts to develop novel α_2 -AR blockers incorporating the arylguanidinium and aryl-2-iminoimidazolidinium structural motifs.

Thus, in order to gain further insight into which structural elements impart α_2 -AR antagonism, we sought to develop a 3D pharmacophore hypothesis using the GALAHAD pharmacophore perception software [20]. By examining a diverse range of α_2 -AR antagonists taken from the literature, we aimed to highlight the features associated with α_2 -AR antagonist activity and to incorporate these structural elements in the design of a new generation of arylguanidinium/aryl-2-iminoimidazolidinium derivatives.

2. Results and discussion

2.1. Computational design

In order to develop a pharmacophore model for α_2 -AR antagonism, we employed the GALAHAD program as implemented in the Sybyl X 1.3 software suite [21]. GALAHAD takes a series of compounds with a common biological activity as input and then uses a genetic algorithm to flexibly align these compounds on the basis of shared pharmacophoric features such as hydrogen bond acceptors or donors, hydrophobic regions, or electronically-charged moieties. The output is a series of 3D pharmacophore models which describe the spatial relationships between the structural elements corresponding to biological activity; these models can then assist in the discovery and design of new compounds which incorporate the desired bioactivity.

We began by selecting a diverse series of ten known α_2 -AR antagonists, including one high-affinity antagonist taken from our previous work [16] (Fig. 2, compound 7), all of which incorporate a characteristic protonated amine moiety. This is a common motif found in many α_2 -AR antagonists and we hoped that it would serve as a central feature in our pharmacophore model which would

allow us to draw analogies between our own series of arylguanidine α_2 -AR ligands and other, structurally distinct, α_2 -AR antagonists.

All 3D structures were generated using the CONCORD program [22], followed by geometry optimisation using the Tripos molecular mechanics force field [23]. In cases where enantiomers are present (i.e. idazoxan and mianserin), both enantiomers were used in the study. The GALAHAD program was then run several times modifying the parameters (see experimental section) until a pharmacophore model matching all ten antagonists (twelve including both enantiomers of idazoxan and mianserin) was determined. Although the program constructed several competing models, we chose this particular one as it represents the only case in which the pharmacophoric elements match satisfactorily with every antagonist molecule in the study. The final optimal model includes four pharmacophoric elements; namely three hydrophobic regions and a central protonated nitrogen (Fig. 3).

It is noteworthy that both enantiomers of idazoxan and compound 7 overlap with only three of the four pharmacophoric elements and neglect to overlap with the hydrophobic region labelled as HY1 (Fig. 3), while every other compound overlaps with all four elements. Moreover, many compounds also incorporate hydrogen-bonding moieties within the HY1 region of chemical space. We reasoned that a new generation of arylguanidine α_2 -AR ligands should benefit from the introduction of hydrophobic and/or hydrogen-bonding features which overlap with the HY1 region of chemical space, thereby hoping to produce a series of compounds with improved antagonist activity and avoiding the mixture of agonist/antagonist activities observed in our previous studies.

This design scheme gives rise to two classes of compounds as potential antagonists, namely *N,N'*-disubstituted arylguanidine and 4-substituted-2-aryliminoimidazolidine derivatives, as represented in Fig. 4. The phenyl ring R^1 substituents can be chosen on the basis of high-affinity α_2 -AR ligands previously prepared by our group [16–18], while the R^2 substituents will be chosen to incorporate various hydrophobic elements and potential hydrogen-bonding moieties in an attempt to take advantage of the putative antagonist binding interactions highlighted by this pharmacophore study.

Introducing examples of these two classes of compounds (including the two enantiomers from one of the 4-substituted-2-iminoimidazolines) into our pharmacophore model using the GALAHAD template alignment mode provided strong support for our design scheme. As before, the R^1 group overlaps with the HY2 region of the pharmacophore, while the newly-introduced R^2 group now occupies the region marked as HY1 (Fig. 5). With this supporting evidence in hand, we proceeded to prepare these compounds and to evaluate their pharmacological potential as α_2 -AR antagonists.

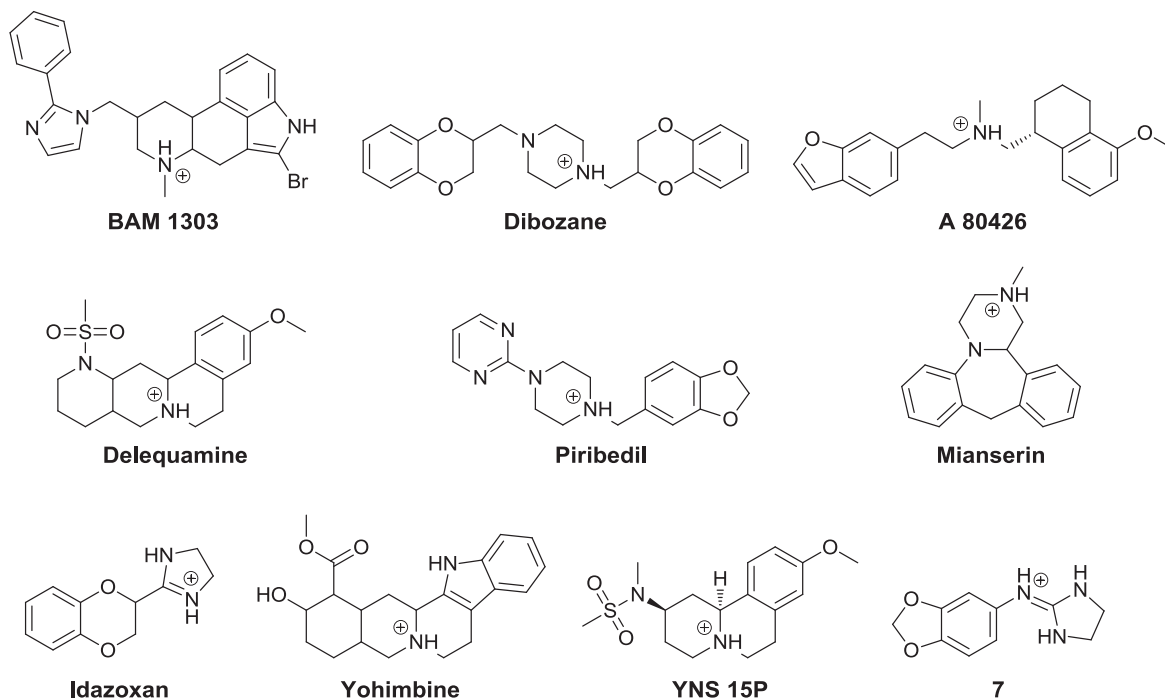


Fig. 2. Structures of α_2 -AR antagonists used in the pharmacophore development study: BAM 1303 [26], Dibozane [26], A-80426 [26], Delaquamine [26], Piribedil [26], Mianserin [26], Idazoxan [26], Yohimbine [26], YNS 15P [26] and compound 7 [16].

2.2. Chemistry

For the preparation of the N,N' -disubstituted arylguanidine series of compounds, we developed a concise three-step procedure to facilitate the rapid preparation of structural analogues (Scheme 1) [24]. Thiourea is first *bis*-Boc protected under standard conditions and then converted *in situ* to the corresponding *N*-Boc protected N' -substituted thioureas **8a–d** by activation with trifluoroacetic anhydride, followed by treatment with the appropriate amine.

The substituted thioureas **8a–d** are then subjected to HgCl_2 promoted guanidylation with an aromatic amine to afford Boc protected N' -substituted arylguanidines **9–13a–d**. Finally, the Boc groups are removed using a methanolic solution of HCl to afford the

final arylguanidine hydrochloride salts **14–18a–d**. For the preparation of compounds with $R^2 = \text{EtOH}$, the alcohol was protected at the thiourea stage as acetate **8b**; the acetate group was cleaved during the Boc deprotection step to afford alcohols **14–18b** (Scheme 1).

The 4-substituted 2-iminoimidazolidine series of compounds were prepared using a similar sequence starting from substituted imidazolidine-2-thiones **19a,b** which were first *bis*-Boc protected under standard conditions (Scheme 2) [25]. Boc protected imidazolidine-2-thiones **20a,b** were then treated with the appropriate aromatic amine in the presence of HgCl_2 and triethylamine to construct the 2-iminoimidazolidine core **21–25a,b**. Finally, the Boc groups were removed using dry HCl in dioxane to afford the

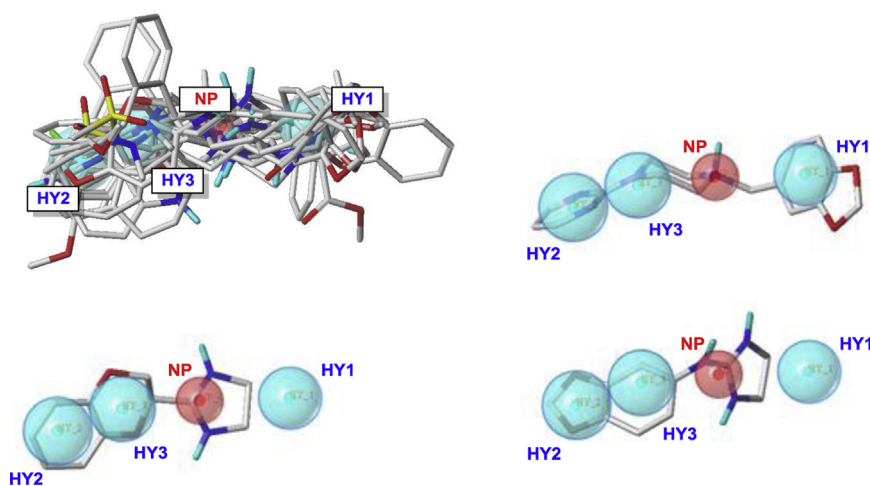


Fig. 3. Final pharmacophore model overlaid with (upper left) all molecules in the study, and the representative α_2 -AR antagonists (upper right) piribedil, (lower left) idazoxan and (lower right) compound 7 with pharmacophoric elements as labelled spheres (HY = hydrophobic region, in blue; NP = protonated nitrogen, in red). The conformations are shown as generated by the GALAHAD program. (For interpretation of the references to colour in this figure legend, the reader is referred to the web version of this article.)

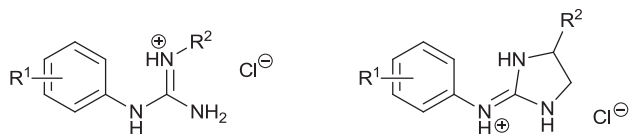


Fig. 4. Proposed structures of potential α_2 -AR antagonists of the N,N' -disubstituted-aryl-guanidine (left) and N -aryl-4-substituted-2-iminoimidazolidine (right) types.

desired 4-substituted-2-iminoimidazolidine hydrochloride salts **26–30a,b**.

2.3. Pharmacology

2.3.1. [3 H]RX821002 competitive binding assays

The affinity of N,N' -disubstituted guanidines **14–18a–d**, plus that of the *mono*-substituted guanidines **14–18e** ($R^2 = H$) towards α_2 -ARs was determined in human prefrontal cortex brain tissue using a competitive binding assay with the α_2 -AR selective radioligand [3 H]RX821002 (2-methoxyidazoxan), which was used at a constant concentration of 2 nM. Affinity data for the guanidine hydrochloride salts **14–18a–e**, calculated as pK_i values, are presented in Table 1; the pK_i values of the clinically-used α_2 -AR agonist clonidine (see structure in Table 1) and the reference ligand RX821002 are included for comparison.

These results outline a number of structure–affinity relationships for arylguanidine α_2 -AR ligands. Broadly speaking, aromatic R^2 substituents (furan-2-ylmethyl and phenyl; **14–18a** and **14–18c**) provide higher affinities on average than non-aromatic groups (ethoxy and *n*-propyl substituents; **14–18b** and **14–18d**). N,N' -disubstituted guanidine derivatives also provide somewhat reduced affinities compared with their *mono*-substituted analogues (**14–18e**). Furthermore, the effect of the R^1 substituent upon affinity loosely follows the order: 1,2,3,4-tetrahydronaphthyl > 4-dimethylamino > 3,4-methylenedioxy > 4-ethylamino > 4-ethoxy. The higher affinities of compounds with the lipophilic $R^1 = 1,2,3,4$ -tetrahydronaphthyl group are in good agreement with our pharmacophore model, in which this moiety overlaps with the hydrophobic regions labelled as HY2 and HY3 (Fig. 3).

Table 2 presents the α_2 -AR affinity data (expressed as pK_i values) for 4-substituted-2-iminoimidazolidine derivatives (**26–30a,b**). As before, the pK_i values of the corresponding unsubstituted 2-iminoimidazolidines (**26c–30c**) [16–18] are included for reference. When compared with the N,N' -disubstituted guanidine series, the substituted 2-iminoimidazolidines generally display lower affinities for the α_2 -AR. This contrasts with previous studies in our group in which unsubstituted 2-iminoimidazolidines ($R^2 = H$) exhibited higher affinities than their unsubstituted guanidine analogues.

The effect of the aryl R^1 substituent loosely follows the same order as observed in the guanidine derivatives: 1,2,3,4-tetrahydronaphthyl > 4-dimethylamino > 3,4-methylenedioxy > 4-ethylamino > 4-ethoxy. Regarding the R^2 substituent, furan derivatives **26–30b** provide higher affinities than their 4-methyl analogues, echoing the higher affinities in furan substituted guanidines **14–18a** versus their *n*-propyl substituted analogues **14–18d**.

In general, the introduction of an R^2 substituent gives rise to slightly lower affinities for the α_2 -AR when compared with our previous series of compounds with $R^2 = H$; this effect is particularly pronounced for the 2-iminoimidazolidine derivatives. Nonetheless, we were eager to determine whether the introduction of the R^2 group prevented activation of α_2 -ARs by fulfilling the requirements of our antagonist pharmacophore model. We therefore proceeded to study the α_2 -AR activity of those compounds with the most promising affinities.

2.3.2. [35 S]GTP γ S binding functional assays

From among the newly-prepared compounds, a set of eleven compounds with the highest affinity towards α_2 -AR (**26c**, **14e**, **15a**, **16c**, **15c**, **16a**, **16d**, **28b**, **28a**, **17a**, **15d**) was subjected to [35 S]GTP γ S binding experiments to determine their effect upon α_2 -ARs as either agonists or antagonists. The α_2 -AR agonist UK14304 (brimonidine) and a selection of five representative compounds with lower affinities (**14a**, **18a**, **15b**, **14d**, **18b**) were also included for comparison.

The [35 S]GTP γ S binding assay is a useful tool to distinguish between agonists, inverse agonists, and antagonists of G-protein coupled receptors such as the α_2 -ARs [26]. When an agonist binds

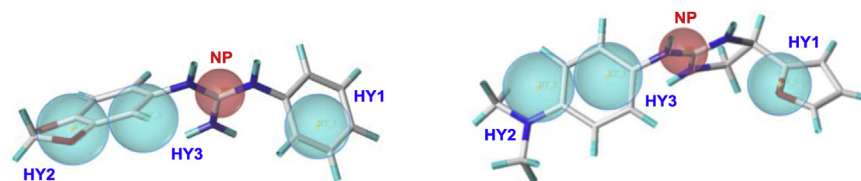
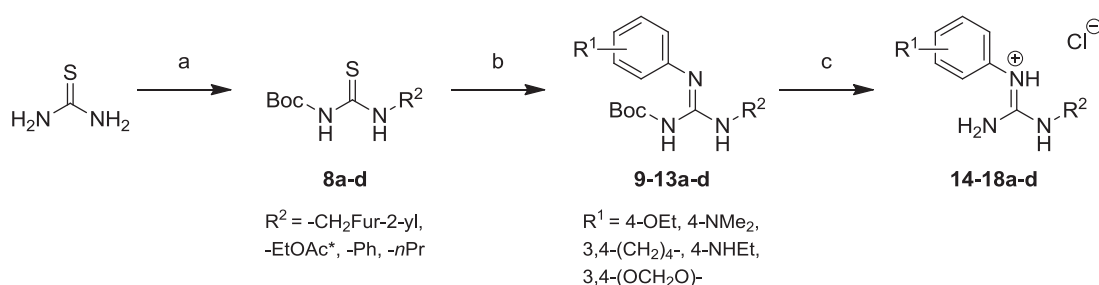
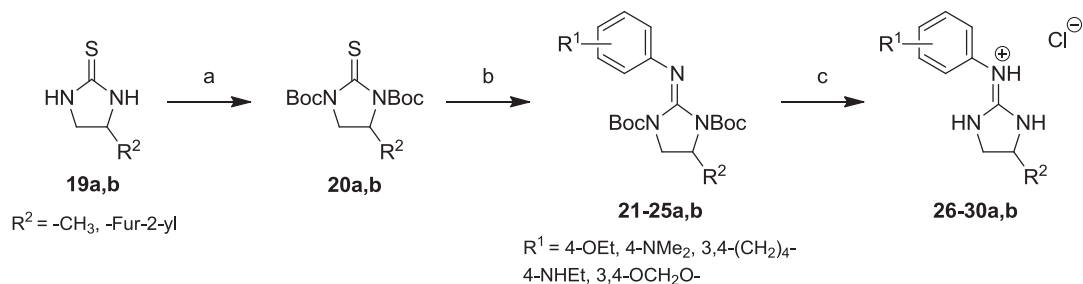


Fig. 5. Pharmacophore model overlaid with two newly-designed compounds; (left) N,N' -disubstituted arylguanidine (**18c**) and (right) N -aryl-4-substituted 2-iminoimidazolidine (**28b**). Compounds are numbered as per Schemes 1 and 2 (*vide infra*).



Scheme 1. Preparation of N,N' -disubstituted arylguanidines. (a) (i) NaH, Boc $_2$ O, THF, 0 °C – rt, 1 h, (ii) NaH, trifluoroacetic anhydride, R $_2$ -NH $_2$, THF, 0 °C – rt, 16 h, 28–91%; (b) HgCl $_2$, TEA, ArNH $_2$, DCM, 0 °C – rt, 16 h, 49–91%; (c) 1.25 M HCl/MeOH, 35 °C, 3.5 h, 65–94%. *The acetate group is removed during step (c), producing **14–18b** with R $_2 = EtOH$.



Scheme 2. Preparation of 4-substituted 2-iminoimidazolidines. (a) NaH, Boc₂O, THF, 0 °C – rt, 3 h, 81–84%; (b) HgCl₂, TEA, ArNH₂, DCM, 0 °C – rt, 16 h 62–88%. (c) 4 M HCl/dioxane, 55 °C, 3.5 h, 58–76%.

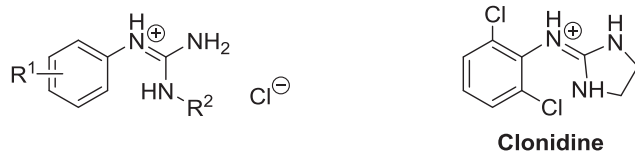
to the α 2-ARs, the conformation of the coupled G protein is altered, leading to the exchange of GDP for GTP on the α -subunit, promoting its dissociation into the α -GTP and $\beta\gamma$ subunits. The activity of the G-protein can be evaluated by determining the guanine nucleotide exchange using radiolabeled GTP analogues. As such, agonists lead to an increase in radio labelled nucleotide binding; inverse agonists lead to a decrease in nucleotide binding, while antagonists exhibit no effect on nucleotide binding. As shown in Fig. 6, all compounds tested showed no stimulatory effect on the [³⁵S]GTP γ S binding, a result which corresponds to antagonist activity.

Five compounds (**14e**, **15a**, **16a**, **16c** and **26c**), which showed high affinities for the α 2-AR in radioligand binding assays and did not stimulate [³⁵S]GTP γ S binding, were further subjected to [³⁵S]GTP γ S

binding experiments in the presence of the α 2-AR selective agonist UK14304 in order to confirm their activity as antagonists. In these experiments, the effect of a set concentration (10⁻⁵ M) of each potential antagonist upon [³⁵S]GTP γ S binding stimulation curves induced by the agonist UK14304 (10⁻¹³ to 10⁻⁴ M) was evaluated. The rightwards shift of the concentration–response curve for UK14304 in the presence of these compounds (Fig. 7) confirmed their α 2-AR antagonist effect.

Thus, the addition of antagonists **14e**, **26c**, **16c**, **15a** and **15c** to [³⁵S]GTP γ S binding experiments induced, in all cases, an increase in the EC₅₀ value for UK14304 (Table 3). In the case of mono-substituted compounds **14e** and **26c** (R¹ = 4-EtO, R² = H), although it remains difficult to rationalise their antagonist effect, it is

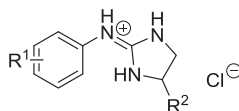
Table 1
Affinity values (expressed as pK_i) obtained for guanidine derivatives **14**–**18a**–**e.2**



Compound	R ¹	R ²	pK _i
RX821002	–	–	8.72
Clonidine	–	–	7.68
14a	4-OEt	–CH ₂ -(fur-2-yl)	5.83
15a	4-NMe ₂	–CH ₂ -(fur-2-yl)	6.67
16a	3,4-(–CH ₂ –) ₄	–CH ₂ -(fur-2-yl)	6.29
17a	4-NHEt	–CH ₂ -(fur-2-yl)	5.97
18a	3,4(–OCH ₂ O–)	–CH ₂ -(fur-2-yl)	5.82
14b	4-OEt	–(CH ₂) ₂ –OH	4.72
15b	4-NMe ₂	–(CH ₂) ₂ –OH	5.73
16b	3,4(–CH ₂ –) ₄	–(CH ₂) ₂ –OH	5.76
17b	4-NHEt	–(CH ₂) ₂ –OH	4.73
18b	3,4(–OCH ₂ O–)	–(CH ₂) ₂ –OH	4.93
14c	4-OEt	–C ₆ H ₅	5.65
15c	4-NMe ₂	–C ₆ H ₅	6.41
16c	3,4(–CH ₂ –) ₄	–C ₆ H ₅	6.58
17c	4-NHEt	–C ₆ H ₅	5.31
18c	3,4(–OCH ₂ O–)	–C ₆ H ₅	5.36
14d	4-OEt	–(CH ₂) ₂ –CH ₃	5.37
15d	4-NMe ₂	–(CH ₂) ₂ –CH ₃	5.95
16d	3,4(–CH ₂ –) ₄	–(CH ₂) ₂ –CH ₃	6.17
17d	4-NHEt	–(CH ₂) ₂ –CH ₃	5.08
18d	3,4(–OCH ₂ O–)	–(CH ₂) ₂ –CH ₃	4.82
14e^a	4-OEt	–H	6.85
15e [18]	4-NMe ₂	–H	7.06
16e [17]	3,4(–CH ₂ –) ₄	–H	7.11
17e [18]	4-NHEt	–H	6.58
18e [16]	3,4(–OCH ₂ O–)	–H	6.40

^a The preparation of compound **14e** is described in the [supplementary material](#).

Table 2
Affinity values (as pK_i) obtained for 2-iminoimidazolidine derivatives **26–30a–c.3**



Compound	R ¹	R ²	pK_i
26a	4-OEt	–CH ₃	4.85
27a	4-NMe ₂	–CH ₃	5.48
28a	3,4-(–CH ₂ –) ₄	–CH ₃	6.00
29a	4-NHEt	–CH ₃	4.91
30a	3,4(–OCH ₂ O–)	–CH ₃	5.63
26b	4-OEt	–(fur-2-yl)	5.58
27b	4-NMe ₂	–(fur-2-yl)	5.88
28b	3,4-(–CH ₂ –) ₄	–(fur-2-yl)	6.16
29b	4-NHEt	–(fur-2-yl)	5.66
30b	3,4(–OCH ₂ O–)	–(fur-2-yl)	5.77
26c^a	4-OEt	–H	7.10
27c [18]	4-NMe ₂	–H	7.42
28c [17]	3,4-(–CH ₂ –) ₄	–H	7.33
29c [18]	4-NHEt	–H	6.75
30c [16]	3,4(–OCH ₂ O–)	–H	7.33

^a The preparation of compound **26c** is described in the [supplementary material](#).

interesting to note that these compounds exhibit a similar shape as the previously discovered guanidine-type antagonist **17e** (R¹ = 4-EtNH, R² = H) [18].

In the case of compound **16c**, the corresponding *mono*-substituted guanidine (compound **3** in Fig. 1) had previously been found to act also as an antagonist [17]. However, the most interesting results are obtained for compounds **15a** and **15c**. In these cases, the corresponding *mono*-substituted guanidine (compound **6** in Fig. 1) was found to act as an agonist [16] and therefore the introduction of the R² substituent (furan-2-ylmethylene for **15a** or phenyl for **15c**) has successfully modified their activity from an α_2 -AR agonist to an antagonist in human brain prefrontal cortex. Although the efficacy of these compounds must still be improved

both in terms of affinity and antagonist potency, there now exists a clear rationale for which structural features can impart antagonist activity within this class of compounds.

3. Conclusions

In our previous studies examining *mono*-substituted guanidine and unsubstituted 2-iminoimidazolidine derivatives, it was often difficult to determine the structure–activity relationships which govern functional activity at the α_2 -AR. Few of these unsubstituted compounds act as antagonists, whereas a significant portion of them acted instead as α_2 -AR agonists.

After a molecular modelling study (using GALAHAD pharmacophore analysis) to inform the design of new α_2 -AR antagonists, a total of 30 new *N,N'*-disubstituted guanidine and 4-substituted 2-iminoimidazolidine derivatives plus 2 new *mono*-substituted guanidine and 4-unsubstituted 2-iminoimidazolidine derivatives were prepared following our previously established synthetic methods.

While the incorporation of the R² substituent seems to lead to a reduction in α_2 -AR affinity as suggested by competitive binding assays in human brain tissue, it is clear from [³⁵S]GTP γ S binding functional experiments that this modification leads to consistent antagonist activity at α_2 -ARs. Clearly, the development of aryl-guanidine α_2 -AR antagonists represents a continuing challenge, as a balance must be struck between the desired antagonist activity imparted by *N,N'*-disubstituted guanidines and the increased receptor affinities associated with their unsubstituted counterparts.

4. Experimental

4.1. Synthesis

All commercial chemicals were obtained from Sigma–Aldrich or Fluka and were used without further purification. Deuterated solvents for NMR use were purchased from Apollo. Dry solvents were prepared using standard procedures, according to Vogel, with distillation prior to use. Chromatographic columns were run using a Biotage SP4 flash purification system with Biotage SNAP silica

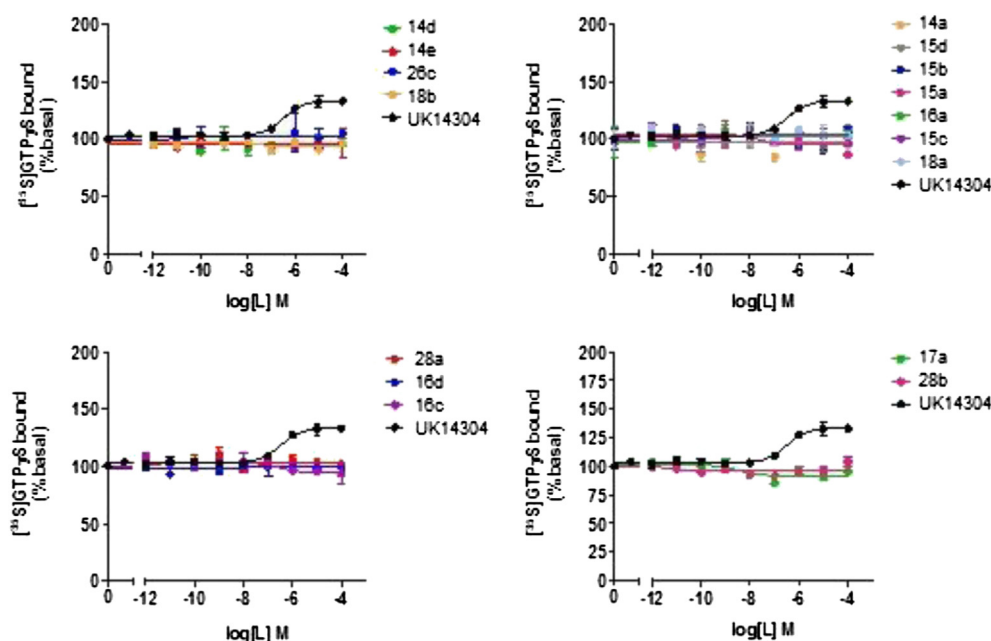


Fig. 6. Dose-response curves for [³⁵S]GTP γ S binding versus ligand concentration.

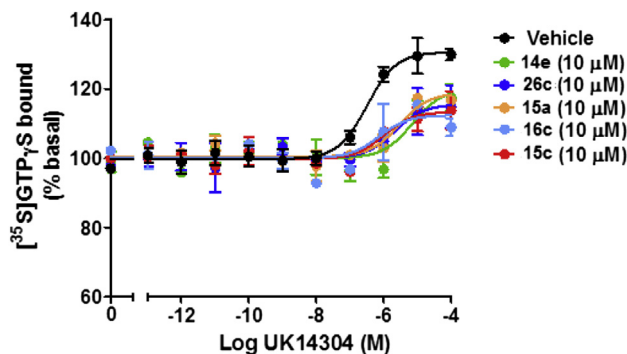


Fig. 7. Dose-response curves for UK14304 stimulation of [^{35}S]GTP γ S binding (10^{-13} to 10^{-4} M, 10 concentrations) in the absence (vehicle) or in the presence of a set concentration (10^{-5} M) of ligands **14e**, **26c**, **15a**, **16c** and **15c**.

cartridges. Solvents for synthesis purposes were used at GPR grade. Analytical TLC was performed using Merck Kieselgel 60 F254 silica gel plates or Polygram Alox N/UV254 aluminium oxide plates. Visualization was by UV light (254 nm). NMR spectra were recorded in a Bruker DPX-400 Avance spectrometer, operating at 400.13 MHz and 600.1 MHz for ^1H NMR; 100.6 MHz and 150.9 MHz for ^{13}C NMR. Shifts are referenced to the internal solvent signals. NMR data were processed using Bruker Win-NMR 5.0 software. HRMS spectra were measured on a Micromass LCT electrospray TOF instrument with a WATERS 2690 autosampler with methanol as carrier solvent. Melting points were determined using a Stuart Scientific Melting Point SMP1 apparatus and are uncorrected. Purity was assessed using reverse phase HPLC with a diode-array detector scanning wavelengths from 200 to 950 nm. HPLC analysis was carried out using a Varian ProStar system equipped with a Varian Prostar 335 diode array detector and a manual injector (20 μL). Integration was performed at 245 nm and peak purity was confirmed using a purity channel. The stationary phase consisted of an ACE 5C18-AR column (150 \times 4.6 mm). The method developed for this type of hydrochloride salts which gave optimum retention times used a gradient from 100% aqueous formate buffer (30 mM, pH 3.0) to 85% formate buffered methanol (30 mM, pH 3.0) and 15% aqueous formate buffer. A minimum purity of 95.0% was set for compounds to be tested pharmacologically.

4.1.1. General methods

4.1.1.1. Method A: general method for the deprotection of N-Boc protected guanidines using trifluoroacetic acid. The Boc protected guanidine (0.73 mmol) was treated with solution of 50% trifluoroacetic acid in methylene chloride (10 mL). After 3 h stirring at room temperature, methylene chloride and trifluoroacetic acid were removed by evaporation, and the residue was dissolved in H_2O (10 mL). To this solution, 1000 mg Amberlite resin in its Cl^- form was added, and the reaction was allowed to proceed overnight. After 16 h the Amberlite was removed by filtration, and the filtrate

Table 3

EC_{50} values obtained from the concentration–response curves for UK14304 stimulation of [^{35}S]GTP γ S binding (10^{-13} – 10^{-4} M, 10 concentrations) in the absence or presence of the different N,N' -disubstituted guanidines (10^{-5} M).

Compound	EC_{50} (μM) \pm SEM
UK14304	0.4 \pm 0.01
UK14304 + 14e	7.0 \pm 0.54
UK14304 + 26c	2.2 \pm 0.17
UK14304 + 16c	0.7 \pm 0.07
UK14304 + 15a	2.8 \pm 0.24
UK14304 + 15c	1.0 \pm 0.10

was washed twice with methylene chloride (2 \times 15 mL). The aqueous phase was evaporated to yield the crude hydrochloride salt. The product was purified by reverse phase chromatography (C-8 silica, typical elution gradient: 100% H_2O to 85:15% H_2O :acetonitrile). Solvents were removed *in vacuo* to afford the product.

4.1.1.2. Method B: general method for the deprotection of N-Boc protected guanidines using methanolic hydrochloric acid. The Boc protected guanidine (0.39 mmol) was dissolved in 1.25 M methanolic HCl and stirred under argon until the reaction was adjudged complete (Note: If the reaction fails to proceed to completion after 3 h by TLC, an additional 0.5 mL conc. HCl may be added to the mixture). At the reaction endpoint, evaporation of solvents and HCl was followed by reverse phase chromatography (C-8 silica, typical elution gradient: 100% H_2O to 85:15% H_2O :acetonitrile). The purified fractions were evaporated to dryness to yield the product.

4.1.1.3. Method C: general method for the deprotection of N,N' -bis-Boc protected 2-iminoimidazolidines using hydrochloric acid in dioxane. The bis-Boc protected 2-iminoimidazolidine (0.26 mmol) was dissolved in methylene chloride (0.8 mL) under argon, to which 4 M HCl in dioxane (0.765 mL, 3.06 mmol) were added. The mixture was stirred at 55 $^\circ\text{C}$ until the reaction was adjudged complete (typically 3 h, adjudged by TLC and MS analysis). At the reaction endpoint, solvents and HCl were evaporated, followed by either of two chromatographic methods. Method 1 comprised of normal phase silica gel chromatography using a solvent system consisting of methylene chloride and 80:20:3 CHCl_3 :MeOH: NH_4OH (CMA), respectively (typical elution gradient: 100% methylene chloride to 1:1 methylene chloride:CMA). The purified fractions were evaporated to dryness, and the residue was dissolved in 1.25 M methanolic HCl (2.5 mL). Evaporation of solvents and HCl gas afforded the product. Method 2 comprised of reverse phase chromatography using C-8 silica, typical elution gradient: 100% H_2O to 85:15% H_2O :acetonitrile, respectively. The purified fractions were evaporated to dryness to afford the product.

4.1.2. N -(4-Ethoxyphenyl)- N' -(furan-2-ylmethyl)guanidine hydrochloride (**14a**)

Following Method B and starting from **9a** (260 mg, 0.73 mmol) the title compound was obtained as a pale yellow hygroscopic solid (110 mg, 51%). Mp: 52–60 $^\circ\text{C}$; ^1H NMR (D_2O): δ 7.48 (app s, 1H, CH–O Fur.), 7.12 (d, J = 8.6 Hz, 2H, CH Ar.), 6.94 (d, J = 8.6 Hz, 2H, CH Ar.), 6.40 (app s, 2H, 2CH Fur.), 4.44 (s, 2H, NHCH_2), 4.02 (q, J = 7.0 Hz, 2H, CH_2CH_3), 1.31 (t, J = 7.0 Hz, 3H, CH_2CH_3); ^{13}C NMR (D_2O): δ 157.2 (Cq Ar.), 155.1 (C=N), 148.7 (Cq Fur.), 142.8 (CH–O, Fur.), 127.5 (CH Ar.), 126.2 (Cq Ar.), 115.3 (CH Ar.), 110.2 (CH Fur.), 107.8 (CH Fur.), 64.0 (CH_2CH_3), 37.6 (NHCH_2), 13.4 (CH_2CH_3); IR (neat, cm^{-1}): $\bar{\nu}$ 3126 (NH), 2979 (CH), 2343, 1619, 1509, 1476, 1394, 1238, 1172 (C–O), 1114 (C–O), 1042; HRMS (m/z ES): Found: 260.1393 (M^+ , $\text{C}_{14}\text{H}_{18}\text{N}_3\text{O}_2$ Requires: 260.1399); Purity by HPLC: 95.1% (t_{R} 25.96 min).

4.1.3. N -[4-(dimethylamino)phenyl]- N' -(furan-2-ylmethyl)guanidine hydrochloride (**15a**)

Following Method B and starting from **10a** (260 mg, 0.72 mmol) the title compound was obtained as an orange hygroscopic solid (122 mg, 57%). Mp: 96–104 $^\circ\text{C}$; ^1H NMR (D_2O): δ 7.66 (d, J = 9.0 Hz, 2H, CH Ar.), 7.46 (app s, 1H, CH–O Fur.), 7.44 (d, J = 9.0 Hz, 2H, CH Ar.), 6.41 (app s, 2H, 2CH Fur.), 4.49 (s, 2H, CH_2), 3.28 (s, 6H, $\text{N}(\text{CH}_3)_2$); ^{13}C NMR (D_2O): δ 154.6 (C=N), 148.4 (Cq Fur.), 142.9 (CH–O Fur.), 139.9 (Cq Ar.), 136.0 (Cq Ar.), 126.4 (CH Ar.), 121.8 (CH Ar.), 110.2 (CH Fur.), 108.0 (CH Fur.), 45.9 ($\text{N}(\text{CH}_3)_2$), 37.9 (CH_2); IR (neat, cm^{-1}): $\bar{\nu}$ 3114 (NH), 2322, 1620, 1584, 1515, 1465, 1374, 1258, 1195, 1133, 1072, 1016; HRMS (m/z ES): Found: 259.1554 (M^+).

$C_{14}H_{19}N_4O$ Requires: 259.1559); Purity by HPLC: 95.7% (t_R 23.55 min).

4.1.4. *N*-(5,6,7,8-tetrahydronaphth-2-yl)-*N'*-(furan-2-ylmethyl)guanidine hydrochloride (**16a**)

Following Method B and starting from **11a** (155 mg, 0.42 mmol) the title compound was obtained as a clear hygroscopic solid (68 mg, 53%). Mp: 72–78 °C; 1H NMR (D_2O): δ 7.48 (m, 1H, CH–O Fur.), 7.13 (d, J = 9.0 Hz, 1H, CH Ar.), 6.92 (m, 2H, 2CH Ar.), 6.41 (dd, J = 3.5, 2.0 Hz, 1H, CH Fur.), 6.38 (d, J = 3.5 Hz, 1H, CH Fur.), 4.44 (s, 2H, $NHCH_2$), 2.68 (m, 4H, 2CH₂), 1.70 (m, 4H, 2CH₂); ^{13}C NMR (D_2O): δ 154.9 (C=N), 148.7 (Cq Fur.), 142.8 (CH–O, Fur.), 138.8 (Cq Ar.), 137.0 (Cq Ar.), 130.6 (Cq Ar.), 130.0 (CH Ar.), 125.8 (CH Ar.), 122.5 (CH Ar.), 110.1 (CH Fur.), 107.7 (CH Fur.), 37.6 ($NHCH_2$), 28.2 (CqCH₂CH₂), 27.9 (CqCH₂CH₂), 22.0 (CqCH₂CH₂), 21.8 (CqCH₂CH₂); IR (neat, cm^{-1}): $\bar{\nu}$ 3143 (NH), 2929 (CH), 2858, 1631, 1600, 1501, 1436, 1346, 1247, 1148, 1074, 1014; HRMS (m/z ES): Found: 270.1608 (M^+). $C_{16}H_{20}N_3O$ Requires: 270.1606); Purity by HPLC: 95.2% (t_R 29.12 min).

4.1.5. *N*-(4-ethylaminophenyl)-*N'*-(furan-2-ylmethyl)guanidine hydrochloride (**17a**)

To a solution of **12a** (90 mg, 0.25 mmol) in a 1:1 mixture of isopropyl alcohol and methylene chloride (630 μ L) was added a 4 M solution of HCl in dioxane (377 μ L, 1.51 mmol). After 3.5 h stirring at 35 °C, solvents were evaporated and the residue was purified by reverse phase chromatography (C-8 silica using a 100% H₂O mobile phase). Removal of solvents *in vacuo* at a temperature not exceeding 35 °C afforded the title compound as a yellow hygroscopic gum (70 mg, 84%). 1H NMR (D_2O): δ 7.49 (d, J = 8.5 Hz, 2H, CH Ar.), 7.48 (app s, 1H, CH–O Fur.), 7.40 (d, J = 8.5 Hz, 2H, CH Ar.), 6.29 (app d, J = 3.0 Hz, 2H, 2CH Fur.), 4.47 (s, 2H, $NHCH_2$), 3.43 (q, J = 7.5 Hz, 2H, CH₂CH₃), 1.27 (t, J = 7.5 Hz, 3H, CH₂CH₃); ^{13}C NMR (D_2O): δ 154.6 (C=N), 148.5 (Cq–O Fur.), 142.9 (CH–O Fur.), 135.6 (Cq Ar.), 132.6 (Cq Ar.), 126.4 (CH Ar.), 123.9 (CH Ar.), 110.1 (CH Fur.), 107.9 (CH Fur.), 46.9 (CH₂CH₃), 37.8 ($NHCH_2$), 9.7 (CH₂CH₃); IR (neat, cm^{-1}): $\bar{\nu}$ 3146 (NH), 2943 (CH), 2477, 1656, 1625, 1590, 1513, 1444, 1148 (C–O), 1105 (C–O), 1018; HRMS (m/z ES): Found: 259.1548 (M^+). $C_{14}H_{19}N_4O$ Requires: 259.1599); Purity by HPLC: 95.7% (t_R 22.12 min).

4.1.6. *N*-(3,4-methylenedioxyphenyl)-*N'*-(furan-2-ylmethyl)guanidine hydrochloride (**18a**)

To a solution of **13a** (165 mg, 0.46 mmol) in methylene chloride (4.0 mL) was added a 4 M solution of HCl in dioxane (689 μ L, 2.76 mmol). After 4.5 h stirring at rt, solvents were evaporated and the residue was purified by reverse phase chromatography (C-8 silica using a 100% H₂O mobile phase). Removal of solvents *in vacuo* at a temperature not exceeding 35 °C afforded the title compound as a yellow hygroscopic solid (88 mg, 65%). Mp: 78–82 °C; 1H NMR (D_2O): δ 7.46 (app s, 1H, CH–O Fur.), 6.84 (d, J = 8.0 Hz, 1H, CH Ar.), 6.73 (s, 1H, CH Ar.), 6.71 (d, J = 8.0 Hz, 1H, CH Ar.), 6.39 (s, 1H, CH Fur.), 6.37 (s, 1H, CH Fur.), 5.96 (s, 2H, OCH₂O), 4.42 (s, 2H, $NHCH_2$); ^{13}C NMR (D_2O): δ 155.2 (C=N), 148.7 (Cq Fur.), 147.5 (Cq Ar.), 146.5 (Cq Ar.), 142.8 (CH–O, Fur.), 126.9 (Cq Ar.), 120.0 (CH Ar.), 110.1 (CH Fur.), 108.4 (CH Ar.), 107.7 (CH Fur.), 107.2 (CH Ar.), 101.4 (OCH₂O), 37.6 ($NHCH_2$); IR (neat, cm^{-1}): $\bar{\nu}$ 3121, 1596 (C=N), 1501, 1486, 1446, 1346, 1246, 1204 (C–O), 1032, 923; HRMS (m/z ES): Found: 260.1032 (M^+). $C_{13}H_{14}N_3O_3$ Requires: 260.1035); Purity by HPLC: 97.0% (t_R 23.79 min).

4.1.7. *N*-(4-Ethoxyphenyl)-*N'*-(2-hydroxyethyl)guanidine hydrochloride (**14b**)

Following Method A and starting from **9b** (60 mg, 0.19 mmol), the title compound was obtained as a brown, very hygroscopic solid

(45 mg, 94%). Mp: 42–46 °C; 1H NMR (D_2O): δ 7.20 (d, J = 8.5 Hz, 2H, CH Ar.), 6.99 (d, J = 8.5 Hz, 2H, CH Ar.), 4.05 (q, J = 7.0 Hz, 2H, CH₂CH₃), 3.69 (t, J = 5.0 Hz, 2H, CH₂OH), 3.36 (t, J = 5.0 Hz, 2H, $NHCH_2$), 1.33 (t, J = 7.0 Hz, 3H, CH₂CH₃); ^{13}C NMR (D_2O): δ 157.1 (Cq Ar.), 155.6 (C=N), 127.5 (CH Ar.), 126.4 (Cq Ar.), 115.2 (CH Ar.), 64.0 (CH₂CH₃), 59.3 (CH₂OH), 43.1 ($NHCH_2$), 13.3 (CH₂CH₃); IR (neat, cm^{-1}): $\bar{\nu}$ 3158 (NH), 2979 (CH), 2368, 1617, 1514, 1476, 1394, 1237, 1171 (C–O), 1114 (C–O), 1042; HRMS (m/z ES): Found: 224.1403 (M^+). $C_{11}H_{18}N_3O_2$ Requires: 224.1399); Purity by HPLC: 96.8% (t_R 21.97 min).

4.1.8. *N*-[4-(dimethylamino)phenyl]-*N'*-(2-hydroxyethyl)guanidine hydrochloride (**15b**)

Following Method A and starting from **10b** (100 mg, 0.31 mmol), the title compound was obtained as an off-white hygroscopic solid (65 mg, 80%). Mp: 54–62 °C; 1H NMR (D_2O): δ 7.68 (d, J = 9.0 Hz, 2H, CH Ar.), 7.49 (d, J = 9.0 Hz, 2H, CH Ar.), 3.74 (t, J = 5.0 Hz, 2H, CH₂OH), 3.44 (t, J = 5.0 Hz, 2H, $NHCH_2$), 3.29 (s, 6H, N(CH₃)₂); ^{13}C NMR (D_2O): δ 155.1 (C=N), 139.8 (Cq Ar.), 136.1 (Cq Ar.), 126.3 (CH Ar.), 121.7 (CH Ar.), 59.4 (CH₂OH), 45.9 (N(CH₃)₂), 43.4 ($NHCH_2$); IR (neat, cm^{-1}): $\bar{\nu}$ 3164 (NH), 2578, 2453, 1662, 1628, 1592, 1516, 1469, 1410, 1260, 1184, 1135, 1063; HRMS (m/z ES): Found: 223.1550 (M^+). $C_{11}H_{19}N_4O$ Requires: 223.1559); Purity by HPLC: 99.3% (t_R 15.76 min).

4.1.9. *N*-(5,6,7,8-tetrahydronaphth-2-yl)-*N'*-(2-hydroxyethyl)guanidine hydrochloride (**16b**)

Following Method A and starting from **11b** (230 mg, 0.61 mmol) the title compound was obtained as a yellow hygroscopic solid (144 mg, 87%). Mp: 64–70 °C; 1H NMR (D_2O): δ 7.04 (d, J = 7.5 Hz, 1H, CH Ar.), 6.88 (d, J = 7.5 Hz, 1H, CH Ar.), 6.87 (s, 1H, CH Ar.), 3.68 (t, J = 5.0 Hz, 2H, CH₂OH), 3.36 (t, J = 5.0 Hz, 2H, $NHCH_2$), 2.60 (m, 4H, 2CH₂), 1.63 (m, 4H, 2CH₂); ^{13}C NMR (D_2O): δ 155.0 (C=N), 138.3 (Cq Ar.), 135.9 (Cq Ar.), 130.8 (Cq Ar.), 129.8 (CH Ar.), 125.0 (CH Ar.), 121.8 (CH Ar.), 59.4 (CH₂OH), 43.2 ($NHCH_2$), 28.3 (CqCH₂CH₂), 28.0 (CqCH₂CH₂), 22.1 (CqCH₂CH₂), 22.0 (CqCH₂CH₂); IR (neat, cm^{-1}): $\bar{\nu}$ 3265 (OH), 3154 (NH), 2928 (CH), 1628, 1601, 1501, 1435, 1352, 1249, 1136, 1062 (C–O); HRMS (m/z ES): Found: 234.1609 (M^+). $C_{13}H_{20}N_3O$ Requires: 234.1606); Purity by HPLC: 95.9% (t_R 26.85 min).

4.1.10. *N*-(4-ethylaminophenyl)-*N'*-(2-hydroxyethyl)guanidine hydrochloride (**17b**)

A solution of **12b** (87 mg, 0.24 mmol) in methanol (1.8 mL) was treated with 35 equivalents of conc. HCl (0.70 mL, 8.40 mmol). After 3 h stirring at 60 °C, the reaction was adjudged complete (TLC, MS), solvents were evaporated, and the residue was purified by reverse phase chromatography (C-8 silica using 100% H₂O mobile phase). Removal of solvents afforded the title compound as an off-white solid (49 mg, 77%). Mp: 172–178 °C; 1H NMR (D_2O): δ 7.49 (d, J = 8.5 Hz, 2H, CH Ar.), 7.42 (d, J = 8.5 Hz, 2H, CH Ar.), 3.70 (t, J = 4.5 Hz, 2H, CH₂OH), 3.42 (m, 4H, 2CH₂), 1.26 (t, 3H, J = 7.0 Hz, CH₂CH₃); ^{13}C NMR (D_2O): δ 155.1 (C=N), 135.7 (Cq Ar.), 132.4 (Cq Ar.), 126.3 (CH Ar.), 123.9 (CH Ar.), 59.3 (CH₂OH), 46.9 (CH₂CH₃), 43.4 ($NHCH_2$), 9.7 (CH₂CH₃); IR (neat, cm^{-1}): $\bar{\nu}$ 3266 (OH), 3161 (NH), 2943 (CH), 2662, 2479, 1660, 1626, 1591, 1513, 1443, 1350, 1252, 1058, 1019; HRMS (m/z ES): Found: 223.1557 (M^+). $C_{11}H_{19}N_4O$ Requires: 223.1559); Purity by HPLC: 98.5% (t_R 7.60 min).

4.1.11. *N*-(3,4-methylenedioxyphenyl)-*N'*-(2-hydroxyethyl)guanidine hydrochloride (**18b**)

Following Method A and starting from **13b** (162 mg, 0.44 mmol) the title compound was obtained as a yellow hygroscopic gum (113 mg, 98%). 1H NMR (D_2O): δ 6.85 (d, J = 7.5 Hz, 1H, CH Ar.), 6.74 (m, 2H, CH Ar.), 5.96 (s, 1H, OCH₂O), 3.70 (t, J = 5.0 Hz, 2H, CH₂OH), 3.37 (t, J = 5.0 Hz, 2H, $NHCH_2$); ^{13}C NMR (D_2O): δ 155.6 (C=N), 147.5

(Cq Ar.), 146.4 (Cq Ar.), 127.1 (Cq Ar.), 119.8 (CH Ar.), 108.4 (CH Ar.), 107.1 (CH Ar.) 101.5 (OCH₂O), 59.4 (CH₂OH), 43.2 (NHCH₂); IR (neat, cm⁻¹): $\bar{\nu}$ 3163, 1602 (C=N), 1501, 1486, 1352, 1245, 1203 (C–O), 1062, 1032; HRMS (*m/z* ES): Found: 224.1030 (M⁺. C₁₀H₁₄N₃O₃ Requires: 224.1035); Purity by HPLC: 96.0% (t_R 18.23 min).

4.1.12. *N*-(4-ethoxyphenyl)-*N'*-phenylguanidine hydrochloride (**14c**)

Following Method A and starting from **9c** (138 mg, 0.39 mmol) the title compound was obtained as an off-white hygroscopic solid (98 mg, 87%). Mp: 48–55 °C; ¹H NMR (D₂O): δ 7.49 (t, *J* = 8.0 Hz, 2H, CH Ar.), 7.41 (t, *J* = 8.0 Hz, 1H, CH Ar.), 7.35 (d, *J* = 8.0 Hz, 2H, CH Ar.), 7.30 (d, *J* = 9.0 Hz, 2H, CH Ar.), 7.04 (d, *J* = 9.0 Hz, 2H, CH Ar.), 4.11 (q, *J* = 7.0 Hz, 2H, CH₂CH₃), 1.37 (t, *J* = 7.0 Hz, 3H, CH₂CH₃); ¹³C NMR (D₂O): δ 157.3 (Cq Ar.), 154.7 (C=N), 133.5 (Cq Ar.), 129.5 (CH Ar.), 127.6 (Cq Ar.), 127.5 (CH Ar.), 126.2 (CH Ar.), 125.4 (CH Ar.), 115.3 (CH Ar.), 64.0 (CH₂CH₃), 13.4 (CH₂CH₃); IR (neat, cm⁻¹): $\bar{\nu}$ 3059 (NH), 2978 (CH), 2929 (CH), 2282, 1738, 1616, 1575 (C=N), 1509 (Aryl), 1498, 1476, 1448, 1393, 1301, 1222, 1172, 1114 (C–O), 1087, 1042; HRMS (*m/z* ES): Found: 256.1439 (M⁺. C₁₅H₁₈N₃O Requires: 256.1450); Purity by HPLC: 98.8% (t_R 25.95 min).

4.1.13. *N*-[4-(dimethylamino)phenyl]-*N'*-phenylguanidine hydrochloride (**15c**)

Following Method A and starting from **10c** (122 mg, 0.35 mmol) the title compound was obtained as an off-white hygroscopic solid (69 mg, 70%). Mp: 112–130 °C; ¹H NMR (D₂O): δ 7.68 (d, *J* = 8.7 Hz, 2H, CH Ar.), 7.53 (d, *J* = 8.7 Hz, 2H, CH Ar.), 7.47 (t, *J* = 7.0 Hz, 2H, CH Ar.), 7.37 (t, *J* = 7.0 Hz, 1H, CH Ar.), 7.33 (d, *J* = 7.0 Hz, 2H, CH Ar.), 3.28 (s, 6H, N(CH₃)₂); ¹³C NMR (D₂O): δ 154.1 (C=N), 140.0 (Cq Ar.), 135.9 (Cq Ar.), 133.4 (Cq Ar.), 129.5 (CH Ar.), 127.6 (CH Ar.), 126.5 (CH Ar.), 125.1 (CH Ar.), 121.7 (CH Ar.), 45.9 (N(CH₃)₂); IR (neat, cm⁻¹): $\bar{\nu}$ 3017 (NH), 2429, 1624, 1575, 1514, 1494, 1232, 1183, 1132, 1019; HRMS (*m/z* ES): Found: 255.1609 (M⁺. C₁₅H₁₉N₄ Requires: 255.1610); Purity by HPLC: 99.1% (t_R 24.07 min).

4.1.14. *N*-(5,6,7,8-tetrahydronaphth-2-yl)-*N'*-phenylguanidine hydrochloride (**16c**)

Following Method A and starting from **11c** (280 mg, 0.77 mmol) the title compound was obtained as a yellow hygroscopic gum. Recrystallisation from warm H₂O provided the purified product as a beige solid (203 mg, 88%). Mp: 154–156 °C; ¹H NMR (D₂O): δ 7.40 (t, *J* = 7.5 Hz, 2H, CH Ar.), 7.35 (t, *J* = 7.5 Hz, 1H, CH Ar.), 7.25 (d, *J* = 7.5 Hz, 2H, CH Ar.), 7.10 (d, *J* = 8.0 Hz, 1H, CH Ar.), 6.96 (d, *J* = 8.0 Hz, 1H, CH Ar.), 6.95 (s, 1H, CH Ar.), 2.65 (br s, 4H, 2CH₂), 1.67 (br s, 4H, 2CH₂); ¹³C NMR (D₂O): δ 154.3 (C=N), 138.7 (Cq Ar.), 136.9 (Cq Ar.), 133.5 (Cq Ar.), 130.6 (Cq Ar.), 130.0 (CH Ar.), 129.5 (CH Ar.), 127.5 (CH Ar.), 125.5 (CH Ar.), 125.2 (CH Ar.), 122.2 (CH Ar.), 28.3 (CqCH₂CH₂), 28.0 (CqCH₂CH₂), 22.0 (CqCH₂CH₂), 21.9 (CqCH₂CH₂); IR (neat, cm⁻¹): $\bar{\nu}$ 3170 (NH), 2928 (CH), 1654, 1629, 1593, 1574, 1496, 1371, 1229, 1163; HRMS (*m/z* ES): Found: 266.1651 (M⁺. C₁₇H₂₀N₃ Requires: 266.1657); Purity by HPLC: 97.3% (t_R 29.43 min).

4.1.15. *N*-(4-ethylaminophenyl)-*N'*-phenylguanidine hydrochloride (**17c**)

Following Method A and starting from **12c** (210 mg, 0.59 mmol) the title compound was obtained as a clear hygroscopic gum (75 mg, 44%); ¹H NMR (D₂O): δ 7.49–7.30 (m, 9H, 9CH Ar.), 3.43 (q, 2H, *J* = 7.0 Hz, CH₂CH₃), 1.26 (t, 3H, *J* = 7.0 Hz, CH₂CH₃); ¹³C NMR (D₂O): δ 154.3 (C=N), 135.5 (Cq Ar.), 133.5 (Cq Ar.), 132.7 (Cq Ar.), 129.5 (CH Ar.), 127.6 (CH Ar.), 126.5 (CH Ar.), 125.2 (CH Ar.), 123.8 (CH Ar.), 46.9 (CH₂CH₃), 9.7 (CH₂CH₃); IR (neat, cm⁻¹): $\bar{\nu}$ 2942 (CH), 2651, 2473, 1655, 1624, 1577, 1513, 1496, 1233, 1104, 1021; HRMS (*m/z* ES): Found: 255.1597 (M⁺. C₁₅H₁₉N₄ Requires: 255.1610); Purity by HPLC: 97.7% (t_R 22.56 min).

4.1.16. *N*-(3,4-methylenedioxyphenyl)-*N'*-phenylguanidine hydrochloride (**18c**)

Following Method A and starting from **13c** (320 mg, 0.90 mmol) the title compound was obtained as an off-white hygroscopic solid (208 mg, 79%). Mp: 96–102 °C; ¹H NMR (D₂O): δ 7.42 (t, *J* = 7.5 Hz, 2H, CH Ar.), 7.36 (t, *J* = 7.5 Hz, 1H, CH phenyl), 7.30 (d, *J* = 7.5 Hz, 2H, CH Ar.), 6.82 (d, *J* = 9.0 Hz, 1H, CH Ar.), 6.76 (s, 1H, CH Ar.), 6.75 (d, *J* = 9.0 Hz, 2H, CH Ar.), 5.91 (s, 1H, OCH₂O); ¹³C NMR (D₂O): δ 154.7 (C=N), 147.5 (Cq Ar.), 146.6 (Cq Ar.), 133.4 (Cq Ar.), 129.5 (CH Ar.), 127.6 (CH Ar.), 126.8 (Cq Ar.), 125.5 (CH Ar.), 119.9 (CH Ar.), 108.4 (CH Ar.), 107.1 (CH Ar.) 101.5 (OCH₂O); IR (neat, cm⁻¹): $\bar{\nu}$ 3129 (NH), 3105 (NH), 2975 (CH), 1619 (C=N), 1580, 1486, 1449, 1244, 1195 (C–O), 1138, 1104, 1032 (C–O), 925; HRMS (*m/z* ES): Found: 256.1082 (M⁺. C₁₄H₁₄N₃O₂ Requires: 256.1086); Purity by HPLC: 99.9% (t_R 23.99 min).

4.1.17. *N*-(4-ethoxyphenyl)-*N'*-propylguanidine hydrochloride (**14d**)

Following Method A and starting from **9d** (108 mg, 0.42 mmol) the title compound was obtained as a yellow hygroscopic solid (90 mg, 83%). Mp: 104–106 °C; ¹H NMR (D₂O): δ 7.22 (d, *J* = 8.5 Hz, 2H, CH Ar.), 7.02 (d, *J* = 8.5 Hz, 2H, CH Ar.), 4.10 (q, *J* = 7.0 Hz, 2H, CH₂CH₃), 3.18 (t, *J* = 7.0 Hz, 2H, CH₂CH₂CH₃), 1.59 (m, 2H, CH₂CH₂CH₃), 1.36 (t, 3H, *J* = 7.0 Hz, CH₂CH₃), 0.91 (t, 3H, *J* = 7.6 Hz, CH₂CH₂CH₃); ¹³C NMR (D₂O): δ 157.1 (Cq Ar.), 155.0 (C=N), 127.6 (CH Ar.), 126.5 (Cq Ar.), 115.3 (CH Ar.), 64.1 (CH₂CH₃), 42.6 (CH₂CH₂CH₃), 21.0 (CH₂CH₂CH₃), 13.4 (CH₂CH₃), 9.9 (CH₂CH₂CH₃); IR (neat, cm⁻¹): $\bar{\nu}$ 3125 (NH), 2964 (CH), 2874, 2367, 1616, 1509, 1474, 1393, 1234, 1172 (C–O), 1112 (C–O), 1047. HRMS (*m/z* ES): Found: 222.1608 (M⁺. C₁₂H₂₀N₃O Requires: 222.1606). Purity by HPLC: 97.9% (t_R 25.19 min).

4.1.18. *N*-[4-(dimethylamino)phenyl]-*N'*-propylguanidine hydrochloride (**15d**)

Following Method A and starting from **10d** (125 mg, 0.39 mmol) the title compound was obtained as a clear hygroscopic solid (65 mg, 65%). Mp: 50–55 °C; ¹H NMR (D₂O): δ 7.68 (d, *J* = 8.6 Hz, 2H, CH Ar.), 7.47 (d, *J* = 8.6 Hz, 2H, CH Ar.), 3.29 (s, 6H, N(CH₃)₂), 3.23 (t, *J* = 6.6 Hz, 2H, CH₂CH₂CH₃), 1.61 (m, 2H, CH₂CH₂CH₃), 0.92 (t, *J* = 7.5 Hz, 3H, CH₂CH₂CH₃); ¹³C NMR (100 MHz, D₂O): δ 154.4 (C=N), 136.7 (Cq Ar.), 136.2 (Cq Ar.), 126.3 (CH Ar.), 121.7 (CH Ar.), 46.0 (N(CH₃)₂), 42.9 (CH₂CH₂CH₃), 20.9 (CH₂CH₂CH₃), 10.0 (CH₂CH₂CH₃); IR (neat, cm⁻¹): $\bar{\nu}$ 3149 (NH), 2465, 2449, 1624, 1591, 1515, 1463, 1260, 1183, 1134, 1017, 995; HRMS (*m/z* ES): Found: 221.1772 (M⁺. C₁₂H₂₁N₄ Requires: 221.1766); Purity by HPLC: 99.4% (t_R 21.52 min).

4.1.19. *N*-(5,6,7,8-tetrahydronaphth-2-yl)-*N'*-propylguanidine hydrochloride (**16d**)

Following Method A and starting from **11a** (230 mg, 0.70 mmol) the title compound was obtained as a yellow hygroscopic gum (135 mg, 73%); ¹H NMR (D₂O): δ 7.08 (d, *J* = 8.0 Hz, 1H, CH Ar.), 6.89 (d, *J* = 8.0 Hz, 1H, CH Ar.), 6.88 (s, 1H, CH Ar.), 3.16 (t, *J* = 7.0 Hz, 2H, CH₂CH₂CH₃), 2.65 (m, 4H, 2CH₂), 1.67 (m, 4H, 2CH₂), 1.56 (m, 2H, CH₂CH₂CH₃), 0.90 (t, *J* = 7.0 Hz, 3H, CH₂CH₂CH₃); ¹³C NMR (D₂O): δ 154.6 (C=N), 138.6 (Cq Ar.), 136.6 (Cq Ar.), 130.8 (Cq Ar.), 129.9 (CH Ar.), 125.5 (CH Ar.), 122.2 (CH Ar.), 42.6 (CH₂CH₂CH₃), 28.3 (CqCH₂CH₂), 28.0 (CqCH₂CH₂), 22.0 (CqCH₂CH₂), 21.9 (CqCH₂CH₂), 21.0 (CH₂CH₂CH₃), 9.9 (CH₂CH₂CH₃); IR (neat, cm⁻¹): $\bar{\nu}$ 3147 (NH), 2930 (CH), 1630, 1602, 1501, 1458, 1436, 1354, 1249, 1135; HRMS (*m/z* ES): Found: 232.1814 (M⁺. C₁₄H₂₂N₃ Requires: 232.1814); Purity by HPLC: 95.1% (t_R 29.19 min).

4.1.20. *N*-(4-ethylaminophenyl)-*N'*-propylguanidine hydrochloride (**17d**)

A solution of **12d** (140 mg, 0.44 mmol) in methanol (3.7 mL) was treated with 60 equivalents of conc. HCl (2.17 mL, 26.25 mmol). After 2 h stirring at 45 °C, the reaction was adjudged complete (TLC, MS), solvents were evaporated, and the residue was purified by reverse phase chromatography (C-8 silica using 100% H₂O mobile phase). Removal of solvents afforded the title compound as a yellow hygroscopic gum (50 mg, 39%). ¹H NMR (D₂O): δ 7.48 (d, *J* = 8.6 Hz, 2H, CH Ar.), 7.40 (d, *J* = 8.6 Hz, 2H, CH Ar.), 3.42 (q, *J* = 7.6 Hz, 2H, CH₂CH₃), 3.18 (t, *J* = 6.5 Hz, 2H, CH₂CH₂CH₃), 1.56 (m, 2H, CH₂CH₂CH₃), 1.25 (t, 3H, *J* = 7.6 Hz, CH₂CH₃), 0.86 (t, *J* = 7.5 Hz, CH₂CH₂CH₃); ¹³C NMR (D₂O): δ 154.5 (C=N), 135.8 (Cq Ar.), 132.4 (Cq Ar.), 126.3 (CH Ar.), 123.8 (CH Ar.), 46.9 (CH₂CH₃), 42.8 (CH₂CH₂CH₃), 20.9 (CH₂CH₂CH₃), 9.9 (CH₂CH₂CH₃), 9.7 (CH₂CH₃); IR (neat, cm⁻¹): ν̄ 3162 (NH), 2966 (CH), 2359, 1621, 1590, 1514, 1455, 1142 (C–O), 1106 (C–O), 1020; HRMS (*m/z* ES): Found: 221.1763 (M⁺. C₁₂H₂₁N₄ Requires: 221.1766); Purity by HPLC: 96.8% (t_R 19.51 min).

4.1.21. *N*-(3,4-methylenedioxyphenyl)-*N'*-propylguanidine hydrochloride (**18d**)

Following Method A and starting from **13d** (250 mg, 0.78 mmol), the title compound was obtained as an off-white hygroscopic solid (145 mg, 85%). Mp: 176–178 °C; ¹H NMR (D₂O): δ 6.80 (d, *J* = 9.0 Hz, 1H, CH Ar.), 6.67 (m, 2H, 2CH Ar.), 5.91 (s, 1H, OCH₂O), 3.11 (t, *J* = 7.0 Hz, 2H, CH₂CH₂CH₃), 1.51 (m, 2H, CH₂CH₂CH₃), 0.85 (t, *J* = 7.0 Hz, 3H, CH₂CH₂CH₃); ¹³C NMR (D₂O): δ 154.9 (C=N), 147.5 (Cq Ar.), 146.3 (Cq Ar.), 127.1 (Cq Ar.), 119.8 (CH Ar.), 108.4 (CH Ar.), 107.1 (CH Ar.), 101.5 (OCH₂O), 42.6 (CH₂CH₂CH₃), 21.0 (CH₂CH₂CH₃), 9.9 (CH₂CH₂CH₃); IR (neat, cm⁻¹): ν̄ 3136 (NH), 2966 (CH), 1638 (C=N), 1622, 1598, 1501, 1486, 1244, 1200 (C–O), 1124 (C–O), 1032; HRMS (*m/z* ES): Found: 222.1239 (M⁺. C₁₁H₁₆N₃O₂ Requires: 222.1243); Purity by HPLC: 97.1% (t_R 22.53 min).

4.1.22. *N*-(4-ethoxyphenyl)guanidine hydrochloride (**14e**)

Following Method A and starting from **9e** (235 mg, 0.62 mmol; see [supporting information](#)) the title compound was obtained without further purification as hygroscopic, off-white solid (120 mg, 90%). Mp: 138–140 °C; ¹H NMR (D₂O): δ 7.16 (d, *J* = 7.5 Hz, 2H, CH Ar.), 6.94 (d, *J* = 7.5 Hz, 2H, CH Ar.), 4.02 (q, *J* = 6.5 Hz, 2H, CH₂CH₃), 1.27 (t, *J* = 6.5 Hz, 3H, CH₂CH₃); ¹³C NMR (D₂O): δ 157.7 (C=N), 156.7 (Cq Ar.), 128.1 (Cq Ar.), 126.9 (CH Ar.), 115.8 (CH Ar.), 64.6 (CH₂CH₃), 13.9 (CH₂CH₃); IR (neat, cm⁻¹): ν̄ 3126 (NH), 2978 (CH), 1663 (C=N), 1619, 1582 (C=N), 1510 (Aryl), 1238, 1114 (C–O), 1041; HRMS (*m/z* ES): Found: 180.1131 (M⁺ + H. C₉H₁₄N₃O Requires: 180.1137); Purity by HPLC: 97.8% (t_R 21.96 min).

4.1.23. 4-Ethoxy-*N*-(4-methylimidazolidin-2-ylidene)aniline hydrochloride (**26a**)

Following Method C and starting from **21a** (170 mg, 0.41 mmol) the title compound was obtained as a clear hygroscopic gum (79 mg, 76%). ¹H NMR (D₂O): δ 7.20 (d, *J* = 9.0 Hz, 2H, CH Ar.), 6.99 (d, *J* = 9.0 Hz, 2H, CH Ar.), 4.15 (m, 1H, CHCH₃), 4.08 (q, *J* = 7.0 Hz, 2H, CH₂CH₃), 3.81 (t, *J* = 9.5 Hz, 1H, CHCH₂), 3.28 (dd, *J* = 9.5, 7.0 Hz, 1H, CHCH₂), 1.34 (t, *J* = 7.0 Hz, 3H, CH₂CH₃), 1.27 (d, *J* = 6.0 Hz, 3H, CHCH₃); ¹³C NMR (D₂O): δ 157.6 (Cq Ar.), 156.8 (C=N), 127.4 (Cq Ar.), 126.2 (CH Ar.), 115.1 (CH Ar.), 64.1 (CH₂CH₃), 51.0 (CHCH₂), 49.0 (CHCH₂), 19.1 (CHCH₃), 13.4 (CH₂CH₃); IR (neat, cm⁻¹): ν̄ 3138 (NH), 2976 (CH), 2931, 1646, 1606, 1586 (C=N), 1511, 1477, 1240, 1175, 1115, 1043, 1011, 922; HRMS (*m/z* ES): Found: 220.1443 (M⁺. C₁₂H₁₈N₃O Requires: 220.1450); Purity by HPLC: 99.3% (t_R 23.91 min).

4.1.24. 4-Dimethylamino-*N*-(4-methylimidazolidin-2-ylidene)aniline hydrochloride (**27a**)

Following Method C and starting from **22a** (201 mg, 0.48 mmol) the title compound was obtained as an off-white hygroscopic gum (99 mg, 71%). ¹H NMR (D₂O): δ 7.66 (d, *J* = 9.0 Hz, 2H, CH Ar.), 7.45 (d, *J* = 9.0 Hz, 2H, CH Ar.), 4.20 (m, 1H, CHCH₃), 3.85 (t, *J* = 10.0 Hz, 1H, CHCH₂), 3.25 (dd, *J* = 10.0, 7.0 Hz, 1H, CHCH₂), 3.27 (s, 6H, N(CH₃)₂), 1.27 (d, *J* = 6.0 Hz, 3H, CHCH₃); ¹³C NMR (D₂O): δ 156.7 (C=N), 139.7 (Cq Ar.), 136.4 (Cq Ar.), 125.1 (CH Ar.), 121.7 (CH Ar.), 51.1 (CHCH₂), 49.1 (CHCH₂), 46.0 (N(CH₃)₂), 19.3 (CHCH₃); IR (neat, cm⁻¹): ν̄ 3127 (NH), 2971 (CH), 1643, 1600, 1517 (C=N), 1380, 1134, 1063, 996; HRMS: (*m/z* ES): Found: 219.1600 (M⁺. C₁₂H₁₉N₄ Requires: 219.1610); Purity by HPLC: 99.0% (t_R 18.83 min).

4.1.25. 2-Amino-*N*-(4-methylimidazolidin-2-ylidene)-5,6,7,8-tetrahydronaphthalene hydrochloride (**28a**)

Following Method C and starting from **23a** (125 mg, 0.29 mmol) the title compound was obtained as a white solid (57 mg, 73%). Mp: 78–82 °C; ¹H NMR (D₂O): δ 7.12 (d, *J* = 8.5 Hz, 1H, CH Ar.), 6.93 (d, *J* = 8.5 Hz, 1H, CH Ar.), 6.92 (s, 1H, CH Ar.), 4.16 (m, 1H, CHCH₃), 3.81 (t, *J* = 9.6 Hz, 1H, CHCH₂), 3.29 (dd, *J* = 9.5 Hz, 7.0 Hz, 1H, CHCH₂), 2.69 (s, 4H, 2CH₂), 1.71 (s, 4H, 2CH₂), 1.27 (d, *J* = 6.0 Hz, 3H, CHCH₃); ¹³C NMR (D₂O): δ 156.9 (C=N), 138.6 (Cq Ar.), 136.2 (Cq Ar.), 131.6 (Cq Ar.), 129.8 (CH Ar.), 123.7 (CH Ar.), 120.5 (CH Ar.), 50.9 (CHCH₃), 49.0 (CHCH₂), 28.3 (CqCH₂CH₂), 27.9 (CqCH₂CH₂), 22.0 (CqCH₂CH₂), 21.9 (CqCH₂CH₂), 19.2 (CHCH₃); IR (neat, cm⁻¹): ν̄ 3148 (NH), 2927 (CH), 1648, 1607, 1581, 1505, 1379, 1338, 1266, 1247, 1135, 1065; HRMS: (*m/z* ES): Found: 230.1651 (M⁺. C₁₄H₂₀N₃ Requires: 230.1657); Purity by HPLC: 98.3% (t_R 26.92 min).

4.1.26. 4-Ethylamino-*N*-(4-methylimidazolidin-2-ylidene)aniline hydrochloride (**29a**)

Following Method C and starting from **24a** (258 mg, 0.62 mmol) the title compound was obtained as a white hygroscopic gum (161 mg, 90%). ¹H NMR (D₂O): δ 7.47 (d, *J* = 8.6 Hz, 2H, CH Ar.), 7.36 (d, *J* = 8.6 Hz, 2H, CH Ar.), 4.13 (m, 1H, CHCH₃), 3.78 (t, *J* = 9.2 Hz, 1H, CHCH₂), 3.39 (q, *J* = 6.8 Hz, 2H, CH₂CH₃), 3.25 (dd, *J* = 9.2, 6.8 Hz, 1H, CHCH₂), 1.21 (app t, *J* = 6.8 Hz, 6H, CHCH₃ + CH₂CH₃); ¹³C NMR (D₂O): δ 156.6 (Cq Ar.), 136.0 (C=N), 132.2 (Cq Ar.), 125.0 (CH Ar.), 123.9 (CH Ar.), 51.1 (CHCH₂), 49.0 (CHCH₂), 47.0 (CH₂CH₃), 19.2 (CHCH₃), 9.8 (CH₂CH₃); IR (neat, cm⁻¹): ν̄ 3146 (NH), 2975 (CH), 2891, 2639, 2464, 1639, 1600, 1514 (C=N), 1446, 1391, 1270; HRMS: (*m/z* ES): Found: 219.1614 (M⁺. C₁₂H₁₉N₄ Requires: 219.1610); Purity by HPLC: 97.9% (t_R 17.71 min).

4.1.27. 5-Amino-*N*-(4-methylimidazolidin-2-ylidene)benzo[d][1,3]dioxole hydrochloride (**30a**)

Following Method C and starting from **25a** (191 mg, 0.46 mmol) the title compound was obtained as a white solid (90 mg, 78%). Mp: 220–222 °C; ¹H NMR (D₂O): δ 6.86 (d, *J* = 8.0 Hz, 1H, CH Ar.), 6.76 (s, 1H, CH Ar.), 6.74 (d, *J* = 8.0 Hz, 1H, CH Ar.), 5.98 (s, 2H, OCH₂O), 4.16 (m, 1H, CHCH₃), 3.81 (t, *J* = 9.5 Hz, 1H, CHCH₂), 3.29 (t, *J* = 7.5 Hz, 1H, CH₂CH), 1.27 (d, *J* = 6.0 Hz, 3H, CHCH₃); ¹³C NMR (D₂O): δ 157.5 (C=N), 147.4 (Cq Ar.), 146.1 (Cq Ar.), 128.0 (Cq Ar.), 118.3 (CH Ar.), 108.2 (CH Ar.), 105.9 (CH Ar.), 101.5 (OCH₂O), 51.0 (CHCH₂), 49.0 (CHCH₂), 19.2 (CHCH₃); IR (neat, cm⁻¹): ν̄ 3248 (NH), 2981 (CH), 2858, 1650, 1605, 1488 (C=N), 1449, 1248, 1198, 1130, 1104, 1032, 925, 809; HRMS: (*m/z* ES): Found: 220.1082 (M⁺. C₁₁H₁₄N₃O₂ Requires: 220.1086); Purity by HPLC: 96.7% (t_R 20.80 min).

4.1.28. 4-Ethoxy-*N*-[4-(*fur*-2-yl)imidazolidin-2-ylidene]aniline hydrochloride (**26b**)

Following Method C and starting from **21b** (140 mg, 0.30 mmol) the title compound was obtained as a clear hygroscopic gum (64 mg, 70%). ¹H NMR (D₂O): δ 7.51 (s, 1H, CH–O Fur.), 7.21 (d,

$J = 8.5$ Hz, 2H, CH Ar.), 6.98 (d, $J = 8.5$ Hz, 2H, CH Ar.), 6.43 (s, 2H, 2 × CH Fur.), 5.21 (dd, $J = 9.5, 6.5$ Hz, 1H, CHCH₂), 4.06 (q, $J = 7.0$ Hz, 2H, CH₂CH₃), 4.04 (app t, $J = 9.5$ Hz, 1H, CHCH₂), 3.81 (dd, $J = 9.5, 6.5$ Hz, 1H, CHCH₂), 1.33 (t, $J = 7.0$ Hz, 3H, CH₂CH₃); ¹³C NMR (D₂O): δ 157.6 (Cq Ar.), 157.0 (C=N), 150.7 (Cq Fur.), 143.2 (CH–O Fur.), 127.1 (Cq Ar.), 126.3 (CH Ar.), 115.2 (CH Ar.), 110.1 (CH Fur.), 107.5 (CH Fur.), 64.0 (CH₂CH₃), 51.5 (CHCH₂), 46.9 (CHCH₂ + CH₂CH₃), 13.4 (CH₂CH₃); IR (neat, cm⁻¹): $\bar{\nu}$ 3119 (NH), 2979 (CH), 1651, 1606, 1586 (C=N), 1512, 1477, 1244, 1043, 1010; HRMS (m/z ES): Found: 272.1397 (M⁺. C₁₅H₁₈N₃O₂ Requires: 272.1399); Purity by HPLC: 97.9% (t_R 25.99 min).

4.1.29. 4-Dimethylamino-N-[4-(fur-2-yl)imidazolidin-2-ylidene]aniline dihydrochloride (27b)

Following Method C and starting from **22b** (80 mg, 0.18 mmol) the title compound was obtained as a hygroscopic off-white solid (33 mg, 58%). Mp: 114–118 °C; ¹H NMR (D₂O): δ 7.67 (d, $J = 8.5$ Hz, 2H, CH Ar.), 7.52 (s, 1H, CH–O Fur.), 7.49 (d, $J = 8.5$ Hz, 2H, CH Ar.), 6.45 (app d, $J = 10.0$ Hz, 2H, 2 × CH Fur.), 5.28 (dd, $J = 10.0, 7.0$ Hz, 1H, CHCH₂), 4.07 (t, $J = 10.0$ Hz, 1H, CHCH₂), 3.87 (dd, $J = 10.0, 7.0$ Hz, 1H, CHCH₂), 3.27 (s, 6H, N(CH₃)₂); ¹³C NMR (D₂O): δ 156.7 (C=N), 150.5 (Cq Fur.), 143.2 (CH–O Fur.), 139.9 (Cq Ar.), 136.2 (Cq Ar.), 125.4 (CH Ar.), 121.7 (CH Ar.), 110.2 (CH Fur.), 107.7 (CH Fur.), 51.6 (CHCH₂), 47.0 (CHCH₂), 45.9 (N(CH₃)₂); IR (neat, cm⁻¹): $\bar{\nu}$ 3120 (NH), 2450 (CH), 1645, 1602 (C=N), 1517, 1332, 1247, 1134, 1015, 902; HRMS (m/z ES): Found: 271.1546 (M⁺. C₁₅H₁₉N₄O Requires: 271.1559); Purity by HPLC: 98.7% (t_R 24.13 min).

4.1.30. 2-Amino-N-[4-(fur-2-yl)imidazolidin-2-ylidene]-5,6,7,8-tetrahydronaphthalene hydrochloride (28b)

Following Method C and starting from **23b** (98 mg, 0.20 mmol) the title compound was obtained as a white solid (39 mg, 60%). Mp: 76–78 °C; ¹H NMR (D₂O): δ 7.51 (s, 1H, CH–O Fur.), 7.15 (d, $J = 8.0$ Hz, 1H, CH Ar.), 7.00 (s, 1H, CH Ar.), 6.99 (d, $J = 8.0$ Hz, 1H, CH Ar.), 6.43 (s, 2H, 2 × CH Fur.), 5.22 (dd, $J = 10.0, 6.5$ Hz, 1H, CHCH₂), 4.02 (t, $J = 10.0$ Hz, 1H, CHCH₂), 3.82 (dd, $J = 10.0, 6.5$ Hz, 1H, CHCH₂), 2.71 (s, 4H, 2 × CH₂), 1.72 (s, 4H, 2 × CH₂); ¹³C NMR (D₂O): δ 157.3 (C=N), 150.7 (Cq Fur.), 143.2 (CH–O Fur.), 138.7 (Cq Ar.), 136.7 (Cq Ar.), 131.4 (Cq Ar.), 129.9 (CH Ar.), 124.3 (CH Ar.), 121.1 (CH Ar.), 110.1 (CH Fur.), 107.5 (CH Fur.), 51.5 (CHCH₂), 46.9 (CHCH₂), 28.3 (CqCH₂CH₂), 27.9 (CqCH₂CH₂), 22.0 (CqCH₂CH₂), 21.8 (CqCH₂CH₂); IR (neat, cm⁻¹): $\bar{\nu}$ 2928 (CH), 1645, 1608 (C=N), 1504, 1435, 1330, 1247, 1193, 1148, 1076, 1011, 907; HRMS (m/z ES): Found: 282.1599 (M⁺. C₁₇H₂₀N₃O Requires: 282.1606); Purity by HPLC: 95.2% (t_R 28.83 min).

4.1.31. 4-Ethylamino-N-[4-(fur-2-yl)imidazolidin-2-ylidene]aniline hydrochloride (29b)

Following Method C and starting from **24b** (122 mg, 0.26 mmol) the title compound was obtained as a peach-coloured solid (78 mg, 77%). Mp: 94–98 °C; ¹H NMR (D₂O): δ 7.52 (m, 3H, CH Fur. + CH Ar.), 7.46 (d, $J = 8.5$ Hz, 2H, CH Ar.), 6.42 (app d, $J = 12.5$ Hz, 2H, CH Fur.), 5.26 (dd, $J = 10.0, 6.5$ Hz, 1H, CHCH₂), 4.04 (t, $J = 10.0$ Hz, 1H, CHCH₂), 3.85 (dd, $J = 10.0, 6.5$ Hz, 1H, CHCH₂), 3.45 (q, $J = 7.5$ Hz, 2H, CH₂CH₃), 1.28 (t, $J = 7.5$ Hz, 3H, CH₂CH₃); ¹³C NMR (D₂O): δ 156.9 (C=N), 150.5 (Cq Fur.), 143.3 (CH–O Fur.), 135.8 (Cq Ar.), 132.6 (Cq Ar.), 125.4 (CH Ar.), 123.9 (CH Ar.), 110.2 (CH Fur.), 107.7 (CH Fur.), 51.5 (CHCH₂), 46.9 (CHCH₂ + CH₂CH₃), 9.7 (CH₂CH₃); IR (neat liquid, cm⁻¹): $\bar{\nu}$ 3113 (NH), 2940 (CH), 2653, 1637, 1599 (C=N), 1514, 1335, 1247, 1148, 1075, 1014; HRMS (m/z ES): Found: 271.1557 (M⁺. C₁₅H₁₉N₄O Requires: 271.1559); Purity by HPLC: 95.4% (t_R 22.63 min).

4.1.32. 5-Amino-N-[4-(fur-2-yl)imidazolidin-2-ylidene]benzo[d][1,3]dioxole hydrochloride (30b)

Following Method C and starting from **25b** (120 mg, 0.25 mmol) the title compound was obtained as a white solid (56 mg, 72%). Mp: 64–68 °C; ¹H NMR (D₂O): δ 7.52 (s, 1H, CH Fur.), 6.87 (d, $J = 8.0$ Hz, 1H, CH Ar.), 6.80 (s, 1H, CH Ar.), 6.78 (d, $J = 8.0$ Hz, 1H, CH Ar.), 6.43 (app d, $J = 1.0$ Hz, 2H, 2 × CH Fur.), 5.99 (s, 2H, OCH₂O), 5.22 (dd, $J = 9.5, 6.5$ Hz, 1H, CHCH₂), 4.02 (t, $J = 9.5$ Hz, 1H, CHCH₂), 3.82 (dd, $J = 9.5, 6.5$ Hz, 1H, CHCH₂); ¹³C NMR (D₂O): δ 157.7 (C=N), 150.7 (Cq Fur.), 147.5 (Cq Ar.), 146.3 (Cq Ar.), 143.2 (CH–O Fur.), 127.7 (Cq Ar.), 118.7 (CH Ar.), 110.1 (CH Fur.), 108.3 (CH Ar.), 107.5 (CH Fur.), 106.2 (CH Ar.), 101.5 (OCH₂O), 51.5 (CHCH₂), 46.9 (CHCH₂); IR (neat, cm⁻¹): $\bar{\nu}$ 3113 (NH), 2898 (CH), 1654, 1626, 1607 (C=N), 1502, 1485, 1450, 1243, 1196, 1033, 926; HRMS (m/z ES): Found: 272.1029 (M⁺. C₁₄H₁₄N₃O₃ Requires: 272.1035); Purity by HPLC: 99.6% (t_R 23.57 min).

4.1.33. N-(4-Ethoxyphenyl)-2-iminoimidazolidine hydrochloride (26c)

Following Method A and starting from **21c** (200 mg, 0.49 mmol; see supporting information) the title compound was obtained without further purification as a hygroscopic, off-white solid (110 mg, 92%). Mp: 142–144 °C; ¹H NMR (D₂O): δ 7.10 (d, $J = 8.7$ Hz, 2H, CH Ar.), 6.89 (d, $J = 8.7$ Hz, 2H, CH Ar.), 3.99 (q, $J = 7.0$ Hz, 2H, CH₂CH₃), 3.60 (s, 4H, CH₂CH₂), 1.26 (t, $J = 7.0$ Hz, 3H, CH₂CH₃); ¹³C NMR (D₂O): δ 159.1 (C=N), 157.3 (Cq Ar.), 127.9 (Cq Ar.), 126.6 (CH Ar.), 115.6 (CH Ar.), 64.5 (CH₂CH₃), 42.7 (CH₂CH₂), 13.8 (CH₂CH₃); IR (neat, cm⁻¹): $\bar{\nu}$ 3134 (NH), 2975 (CH), 2878, 1646, 1621 (C=N), 1512 (Aryl), 1488, 1394, 1293, 1238, 1174, 1116 (C–O), 1083, 1045; HRMS (m/z ES): Found: 206.1294 (M⁺ + H. C₁₁H₁₆N₃O Requires: 206.1293); Purity by HPLC: 98.7% (t_R 23.09 min).

4.2. Pharmacology

4.2.1. Preparation of membranes

Neural membranes (P2 fractions) were prepared from the prefrontal cortex of human brain tissue obtained at autopsy in the Instituto Vasco de Medicina Legal, Bilbao, Spain. Postmortem human brain samples of each subject (~1 g) were homogenized using a Teflon-glass grinder (10 up-and-down strokes at 1500 rpm) in 30 volumes of homogenization buffer (5 mM Tris–HCl, pH 7.4) supplemented with 0.25 M sucrose. The crude homogenate was centrifuged for 5 min at 1000 × g (4 °C), and the supernatant was centrifuged again for 10 min at 40,000 × g (4 °C). The resultant pellet was washed twice in 20 volumes of homogenization buffer and re-centrifuged in similar conditions. Aliquots of 1 mg protein were stored at –70 °C until assay. Protein content was measured according to the Bradford method using BSA as standard and was similar in the different brain samples.

4.2.2. [³H]RX821002 binding assays

Specific [³H]RX821002 binding was measured in 0.25 mL aliquots (50 mM Tris–HCl, pH 7.5) of the neural membranes, which were incubated in 96-well plates with [³H]RX821002 (2 nM) for 30 min at 25 °C in the absence or presence of the competing compounds (10⁻¹² M–10⁻³ M, 10 concentrations). Non-specific binding was determined in the presence of 10 μM adrenaline. Specific binding was determined and plotted as a function of the compound concentration. Incubations were terminated by separating free ligand from bound ligand by rapid filtration under vacuum (1450 Filter Mate Harvester, Perkin Elmer) through GF/C glass fibre filters. The filters were then rinsed three times with 300 μL binding buffer, air-dried (60 min), and counted for radioactivity by liquid scintillation spectrometry using a MicroBeta TriLux counter (Perkin Elmer).

4.2.3. Analysis of binding data

Analysis of competition experiments to obtain the inhibition constant (K_i) were performed by nonlinear regression using the GraphPad Prism program. All experiments were analysed assuming a one-site model of radioligand binding. K_i values were normalized to pK_i values.

4.2.4. [^{35}S]GTP γ S binding assays

The incubation buffer for measuring [^{35}S]GTP γ S binding to brain membranes contained, in a total volume of 250 μL , 1 mM EGTA, 3 mM MgCl_2 , 100 mM NaCl, 50 mM GDP, 50 mM Tris–HCl at pH 7.4, and 0.5 nM [^{35}S]GTP γ S. Protein aliquots were thawed and resuspended in the same buffer. The incubation was started by addition of the membrane suspension (20 μg of membrane proteins) to the previous mixture and was performed at 30 $^\circ\text{C}$ for 120 min with shaking. To evaluate the influence of the compounds on [^{35}S]GTP γ S binding, nine concentrations (10^{-12} to 10^{-4} M) of the compounds were added to the assay. Incubations were terminated by separating free ligand from bound ligand by rapid filtration under vacuum (1450 Filter Mate Harvester, Perkin Elmer) through GF/C glass fibre filters. The filters were then rinsed three times with 300 μL incubation buffer, air-dried (60 min), and the radioactivity trapped was determined by liquid scintillation spectrometry (MicroBeta TriLux counter, Perkin Elmer). The [^{35}S]GTP γ S bound was about 7–14% of the total [^{35}S]GTP γ S added. Nonspecific binding of the radioligand was defined as the remaining [^{35}S]GTP γ S binding in the presence of 10 μM unlabelled GTP γ S.

4.2.5. Analysis of [^{35}S]GTP γ S binding data

The pharmacological parameters of the stimulation curves of the [^{35}S]GTP γ S binding were obtained by non-linear analysis using GraphPad Prism™ software version 5.0.

4.2.6. Drug compounds

[^3H]RX821002 (specific activity 55 Ci mmol^{-1}) was obtained from Amersham International, U.K. [^{35}S]GTP γ S (1250 Ci mmol^{-1}) was purchased from Perkin Elmer Life Sciences (Massachusetts, USA). Clonidine HCl, GDP, GTP, GTP γ S, RX821002 HCl, and UK14304 were purchased from Sigma (St. Louis, U.S.A.). All other chemicals were of the highest purity commercially available.

4.3. Computational methods

The three-dimensional structures of all compounds were generated and optimised using the Tripos molecular mechanical force field [23] as implemented in the Sybyl molecular modelling environment [21] with the Powell conjugate gradient method and a convergence criterion of 0.05 kcal mol^{-1} \AA^{-1} . The GALAHAD program was run using the twelve compounds shown in Fig. 2, initially using the program default parameters and gradually increasing the population size and maximum generations until a satisfactory model was found. The final model was found using a population size of 150 with the maximum generations set to 60 and was the only model found which included all twelve compounds as hits. New designs were tested for overlap with the resulting pharmacophore model by using the GALAHAD program with the “align molecules to template individually” setting engaged, using a population size of 60 with the maximum generations set to 30.

Acknowledgements

The authors are grateful to the Irish Research Council for a postgraduate scholarship (D.H.O'D.) and are indebted to Dr. John O'Brien for NMR studies. C.M. is recipient of a predoctoral fellowship from the University of the Basque Country (UPV/EHU). This

work was also supported by grants from Gobierno Vasco (ITG16-13; SAIOTEK S-PE10UN14), the University of the Basque Country (UFI 11/35) and the Instituto de Salud Carlos III, Centro de Investigación Biomédica en Red de Salud Mental, CIBERSAM.

Appendix A. Supplementary data

Supplementary data related to this article can be found at <http://dx.doi.org/10.1016/j.ejmech.2014.05.057>.

References

- [1] The Global Burden of Disease, 2004 Update, WHO Press, Geneva, 2008.
- [2] Among others: (a) J.J. Schildkraut, The catecholamine hypothesis of affective disorders: a review of supporting evidence, *Am. J. Psychiatry* 122 (1965) 509–522; (b) W.E. Bunney, J.M. Davis, Norepinephrine in depressive reactions, *Arch. Gen. Psychiatry* 13 (1965) 483–494; (c) A. Carlsson, H. Corrodi, K. Fuxe, T. Hokfelt, Effect of antidepressant drugs on the depletion of intraneuronal brain 5-hydroxytryptamine stores caused by 4-methyl- α -ethyl-meta-tyramine, *Eur. J. Pharmacol.* 5 (1969) 357–373.
- [3] M.J. Owens, Molecular and cellular mechanisms of antidepressant drugs, *Depress. Anxiety* 4 (1998) 153–159.
- [4] A.U. Trendelenburg, M. Philipp, A. Meyer, W. Klebroff, L. Hein, K. Starke, All three alpha2-adrenoceptor types serve as autoreceptors in postganglionic sympathetic neurons, *Naunyn Schmiedeb. Arch. Pharmacol.* 368 (2003) 504–512.
- [5] R.W. Invernizzi, S. Garattini, Role of presynaptic alpha2-adrenoceptors in antidepressant action: recent findings from microdialysis studies, *Prog Neuropsychopharmacol Biol Psychiatry* 28 (2004) 819–827.
- [6] H.T. Zhang, L.R. Whisler, Y. Huang, Y. Xiang, J.M. O'Donnell, Postsynaptic alpha-2 adrenergic receptors are critical for the antidepressant-like effects of desipramine on behavior, *Neuropsychopharmacology* 34 (2009) 1067–1077.
- [7] O. Berton, E.J. Nestler, New approaches to antidepressant drug discovery: beyond monoamines, *Nat. Rev. Neurosci.* 7 (2006) 137–151.
- [8] S.U. Yanpallewar, K. Fernandes, S.V. Marathe, K.C. Vadodaria, D. Jhaveri, K. Rommelfanger, U. Ladiwala, S. Jha, V. Muthig, L. Hein, P. Bartlett, D. Weinschenker, V.A. Vaidya, α 2-Adrenoceptor blockade accelerates the neurogenic, neurotrophic, and behavioral effects of chronic antidepressant treatment, *J. Neurosci.* 30 (2010) 1096–1109.
- [9] A.M. González, J. Pascual, J.J. Meana, F. Barturen, C. del Arco, A. Pazos, Autoradiographic demonstration of increased α 2-adrenoceptor agonist binding sites in the hippocampus and frontal cortex of depressed suicide victims, *J. Neurochem.* 63 (1994) 256–265.
- [10] E. Korb, C.L. Wilkinson, R.N. Delgado, K.L. Lovero, S. Finkbeiner, Arc in the nucleus regulates pml-dependent glul1 transcription and homeostatic plasticity, *Nat. Neurosci.* 16 (2013) 874–883.
- [11] F. Serres, M. Rodriguez, J.-M. Rivet, J.-P. Galizzi, B. Lockhart, T. Sharp, M.J. Millan, Blockade of α 2-adrenoceptors induces arc gene expression in rat brain in a glutamate receptor-dependent manner: a combined QPCR, in situ hybridisation and immunocytochemistry study, *Neuropharmacology* 63 (2012) 992–1001.
- [12] D. Healy, *The Antidepressant Era*, Harvard University Press, London, U.K, 1998.
- [13] R.D. Robson, M.J. Antonaccio, J.K. Saelens, J. Liebman, Antagonism by mianserin and classical α -adrenoceptor blocking drugs of some cardiovascular and behavioral effects of clonidine, *Eur. J. Pharmacol.* 47 (1978) 431–442.
- [14] E.H. Kang, I.S. Lee, S.K. Chung, S.Y. Lee, E.J. Kim, J.P. Hong, K.S. Oh, J.M. Woo, S. Kim, J.E. Park, B.H. Yu, Mirtazapine versus venlafaxine for the treatment of somatic symptoms associated with major depressive disorder: a randomized, open-labeled trial, *Psychiatry Res.* 169 (2009) 118–123.
- [15] J.E. Ortega, B. Fernández-Pastor, L.F. Callado, J.J. Meana, In vivo potentiation of reboxetine and citalopram effect on extracellular noradrenaline in rat brain by the α 2-adrenoceptor antagonist RS79948, *Eur. Neuropsychopharmacol.* 20 (2010) 813–822.
- [16] F. Rodriguez, I. Rozas, J.E. Ortega, J.J. Meana, L.F. Callado, Guanidine and 2-aminoimidazole aromatic derivatives as α 2-adrenoceptor antagonists, 1: towards new antidepressants with heteroatomic linkers, *J. Med. Chem.* 50 (2007) 4516–4527.
- [17] F. Rodriguez, I. Rozas, J.E. Ortega, A.M. Erdozain, J.J. Meana, L.F. Callado, Guanidine and 2-aminoimidazole aromatic derivatives as α 2-adrenoceptor antagonists, 2: exploring aliphatic linkers, *J. Med. Chem.* 51 (2008) 3304–3312.
- [18] F. Rodriguez, I. Rozas, A.M. Erdozain, J.J. Meana, L.F. Callado, Guanidine and 2-aminoimidazole aromatic derivatives as potential antidepressants, 3: α 2-adrenoceptor agonism vs antagonism. Structure activity relationships, *J. Med. Chem.* 52 (2009) 601–609.
- [19] C. Muguruza, F. Rodriguez, I. Rozas, J.J. Meana, L. Uriguén, L.F. Callado, Antidepressant-like properties of three new alpha2-adrenoceptor antagonists, *Neuropharmacology* 65 (2013) 13–19.

- [20] N.J. Richmond, C.A. Abram, P.R. Wolohan, E. Abrahamian, P. Willett, R.D. Clark, GALAHAD: 1. Pharmacophore identification by hypermolecular alignment of ligands in 3D, *J. Comput. Aid. Mol. Des.* 20 (2006) 567–587.
- [21] Sybyl X 1.3 is available from Tripos International L.P., St. Louis, MO 63144–72319 USA.
- [22] R.S. Pearlman, Rapid generation of high quality approximate 3D molecular structures, *Chem. Des. Autom. News* 2 (1987) 5–6.
- [23] M. Clark, R.D. Cramer III, N. van Opdenbosch, Validation of the general purpose Tripos e 5.2 force field, *J. Comp. Chem.* 10 (1989) 982–1012.
- [24] D.H. O'Donovan, I. Rozas, A concise synthesis of asymmetrically *N,N'*-disubstituted guanidine, *Tetrahedron Lett.* 52 (2011) 4117–4119.
- [25] D.H. O'Donovan, I. Rozas, New methods for the preparation of aryl 2-iminoimidazolines, *Tetrahedron Lett.* 53 (2012) 4532–4535.
- [26] J. Gonzalez-Maeso, R. Rodriguez-Puertas, A.M. Gabilondo, J.J. Meana, Characterization of receptor-mediated [³⁵S]GTPγS binding to cortical membranes from postmortem human brain, *Eur. J. Pharmacol.* 390 (2000) 25–36.